RADIOLARIAN BIOSTRATIGRAPHY OF THE NORTHERN ALBANIA OPHIOLITES: NEW DATA FROM THE SUB-OPHIOLITIC MÉLANGE AND EASTERN MIRDITA OPHIOLITES

Marco Chiari*,✉, Emilio Saccani, Mensi Prela***, Valerio Bortolotti°, Marta Marcucci°** and **Atsushi Matsuoka°°**

* *C.N.R. - Institute of Geosciences and Earth Resources, Florence, Italy.*
** *Department of Physics and Earth Sciences, Ferrara, Italy.*
*** *Polytechnic University of Tirana, Earth Sciences Department, Tirana, Albania.*
° *Department of Earth Sciences, Florence, Italy.*
°° *Department of Geology, Niigata University, Japan.*
✉ *Corresponding author, email: marco.chiari@igg.cnr.it*

Keywords: *Tethyan ophiolites; Supra-subduction zone; Radiolaria; Jurassic; Albania.*

ABSTRACT

In this paper we present new data on the Jurassic radiolarian assemblages collected in seven sections of the sedimentary cover of the Mirdita ophiolites in Albania. These ophiolites form an outstanding NNW-SSE trending ophiolitic belt representing the remnants of the Mesozoic Neo-Tethyan oceanic lithosphere in the Mediterranean area.

The studied sections were sampled in the sub-ophiolitic mélange of the Western Mirdita ophiolites (Rubik Complex) and in the Eastern Mirdita ophiolitic sequences. In the sub-ophiolitic mélange the oldest ages of radiolarians associated with the basalts are referable to the UAZ 4-5 (late Bajocian to latest Bajocian-early Bathonian) and UAZ 5 (latest Bajocian-early Bathonian). In the radiolarian cherts belonging to the Eastern Mirdita ophiolites similar ages were found: from UAZ 5 (latest Bajocian-early Bathonian) to UAZ 5-7 (latest Bajocian-early Bathonian to late Bathonian-early Callovian).

These new biostratigraphic ages are consistent with the tectono-magmatic evolution of the Jurassic Neo-Tethys. In fact, the UAZ 4-5 and UAZ 5 correspond to the very early stages of subduction initiation, whereas the slightly younger UAZ 5 and UAZ 5-7 ages found in the Eastern Mirdita ophiolites could correspond to the subsequent mature stage of the subduction.

INTRODUCTION

In this paper we studied the sedimentary cover of the Mirdita ophiolites, which form an outstanding NNW-SSE trending ophiolitic belt, which crops out within the Dinaride-Hellenide orogenic belt and represents the remnants of the Mesozoic Neo-Tethyan oceanic lithosphere in the Central Mediterranean area. The Mirdita ophiolites are a key element of the Dinaride-Albanide-Hellenide orogenic belt (Fig. 1), as are made up of complete ophiolite sequences (i.e., oceanic lithospheric sequences from the upper mantle to the lower crust, and upper crust). In north Albania, the ophiolitic belt has been classically subdivided into the Western (WMO) and Eastern (EMO) Mirdita Ophiolites (Shallo, 1994; Beccaluva et al., 1994; Figs. 1, 2). Recent works show that this distinction can be made based on the composition of the mantle sequences, whereas the composition of the magmatic rocks shows a gradual transition from the WMO to the EMO (Saccani et al., 2004; 2011; 2017; Dilek et al., 2005; Bortolotti et al., 2013). Both the WMO and EMO share the same amphibolitic sole and sub-ophiolitic mélange at their bases (Carosi et al., 1996; Saccani et al., 2004; Gaggero et al., 2009; Bortolotti et al., 2013; Myhill, 2011). Likewise, both ophiolites share the same supra-ophiolitic mélange (Simoni Mélange) and post-emplacement deposits (Bortolotti et al., 2013). Radiolarian biostratigraphy is a fundamental tool for dating the siliceous sedimentary cover of the ophiolitic volcanic series and when coupled with the geochemistry of the associated volcanics, allow the reconstruction of the geodynamic evolution of the Dinaric-Hellenic belt to be made. In the last 30 years several researches were aimed at dating the cherts in Albania and the first papers were published in the early 1990s (Marcucci et al., 1992; 1994; Chiari et al., 1994; Kellici et al., 1994; Prela et al., 1994).

We present here new data on the Jurassic radiolarian assemblages collected in seven sections in northern Albania (Fig. 1). Four sections are located in the sub-ophiolitic mélange (Rubik Complex; Bortolotti et al., 2013) of the WMO, whereas three sections were sampled in the upper part of the EMO sequences. Some of the radiolarian cherts studied in this paper were stratigraphically associated with volcanic rocks, which were however not studied because of their very intense alteration, which hampered us to unequivocally date the different magmatic events recorded in the Mirdita ophiolites. Nonetheless, we will use regional-scale comparisons and available literature data to tentatively associate the obtained biostratigraphic ages with the magmatic evolution of the Jurassic Neo-Tethys.

GEOLOGICAL SETTING

The Dinaride-Albanide-Hellenide belt formed as a result of the diachronous collision of the Adria plate with Eurasia in Cenozoic times (Dilek et al., 2005). The central-southern segment of this belt (i.e. from Albania to Greece) consists of a series of a stack of tectonic units formed in three distinct domains that are, from west to east (Fig. 1): 1) the rifted continental margin of Adria, composed of a west-vergent imbricate stack of several tectonic units that were classically distinguished with different names in Albania and Greece (see Shallo, 1994; Robertson, 1994; Bortolotti et al., 2013 for an exhaustive description); 2) a Neo-Tethyan oceanic domain represented by an ophiolitic suture that has classically been subdivided into

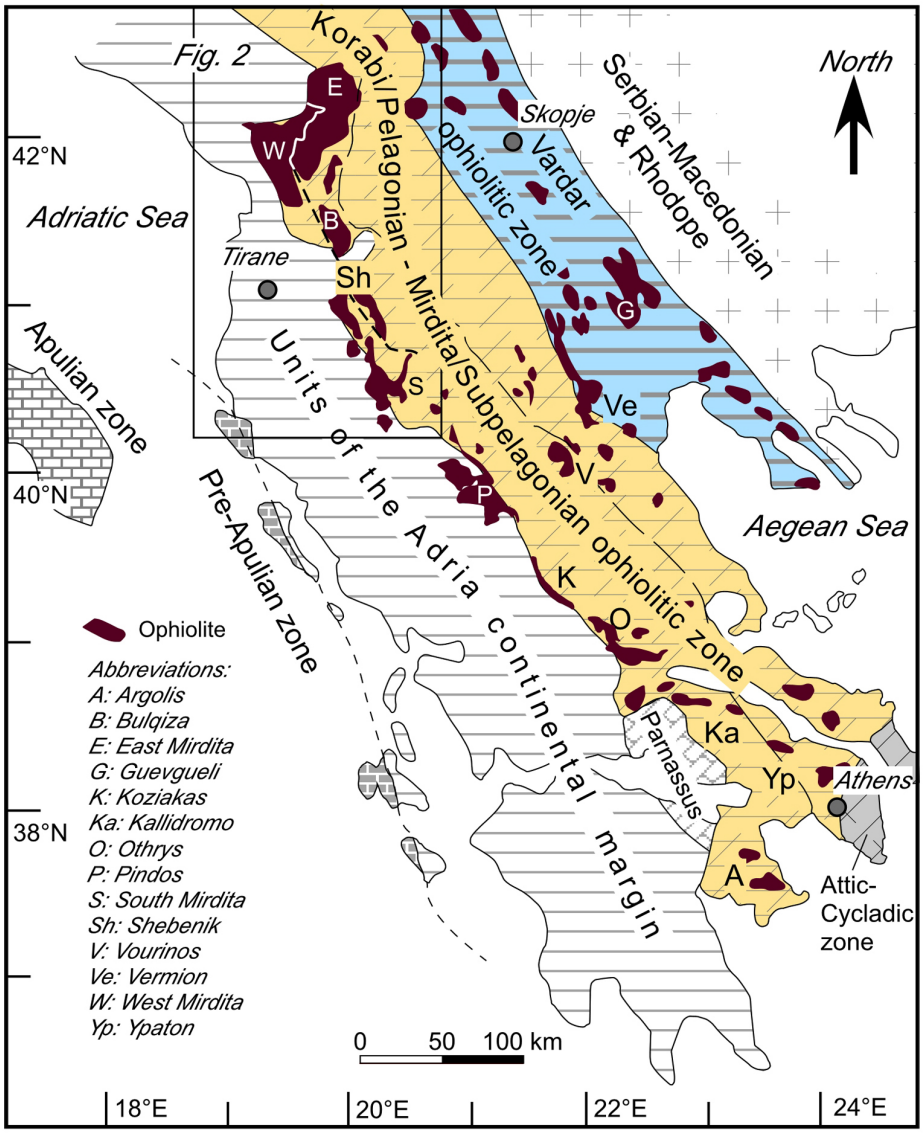

Fig. 1 - Simplified tectonic map of the Albanide-Hellenide orogenic belt showing the main paleo-tectonic domains and the main ophiolitic massifs. Compiled after Ferrière et al. (2012) and Bortolotti et al. (2013). The dashed line indicates the approximate boundary between the Western-type (W) and Eastern-type (E) ophiolites. The box shows the area expanded in Fig. 2.

the Mirdita-Subpelagonian, Korabi-Pelagonian, and Vardar ophiolites (Robertson 1994; Robertson and Shallo, 2000; Dilek et al., 2005; Ferrière et al., 2012); 3) the Serbian-Macedonian and Rhodope continental blocks with Eurasia affinities. In Albania, the orogenic belt includes, from west to east (Fig. 2): 1) the Sazani, Ionian, Kruja, Krasta-Cukali, and Albanian Alps tectonic units representing the Adria continental domain; 2) the Mirdita ophiolites; 3) the Korabi tectonic unit representing the easternmost edge of the Adria continental domain (Bortolotti et al., 2013). Alternatively, some authors refer the Korabi tectonic unit to the western border of an independent microcontinental block known as the Korabi-Pelagonian microcontinent (e.g., Robertson, 1994; Robertson and Shallo, 2000; Shallo and Dilek, 2003; Dilek et al., 2005).

In north Albania, both the WMO and EMO consist of complete Jurassic oceanic lithospheric sequences including a large variety of rocks. It is worth to note that the North Mirdita ophiolites represent, together with the Vourinos ophiolites in Greece, the only preserved complete oceanic sequences in the Albanide-Hellenide belt. According to a classical subdivision of the Mirdita ophiolites, the WMO and EMO were interpreted as representing mid-ocean ridge (MOR) and supra-subduction zone (SSZ) oceanic sequences, respectively (Shallo et al., 1987; Shallo, 1994; Beccaluva et al., 1994). However, many authors showed that although mainly composed of MOR-type rocks, the WMO also include significant amounts of rocks formed in a SSZ setting, whereas minor volumes of typical MOR-type plutonic rocks are interlayered within the SSZ-type intrusive sequences of the EMO (e.g., Bortolotti et al., 1996; 2002; Manika et al., 1997; Bébien et al., 1998; 2000; Insergueix-Filippi et al., 2000; Hoeck et al., 2002; Koller et al., 2006; Saccani et al., 2011; 2017; Saccani and Tassinari, 2015). In addition, the Mirdita ophiolites also include minor Triassic ophiolitic sequences representing portions of the Triassic Vardar ocean basin. They are known as the Porava Unit and consist of slices of pillow basalts showing thin intercalations or covers of red ribbon cherts and rare serpentinite bodies at the base. Pillow basalts range in composition from N-MORBs to alkaline ocean island basalts (Bortolotti et al., 2004) with ages ranging from Middle to Late Triassic (Kellici et al., 1994; Marcucci et al., 1994; Chiari et al., 1996; Bortolotti et al., 2004; 2006; Gawlick et al., 2008).

Generalized stratigraphic reconstructions that resume evidence from different localities of the Mirdita ophiolites are shown in Fig. 3. Both the WMO and EMO are associated throughout with the same sub-ophiolitic mélange unit (the

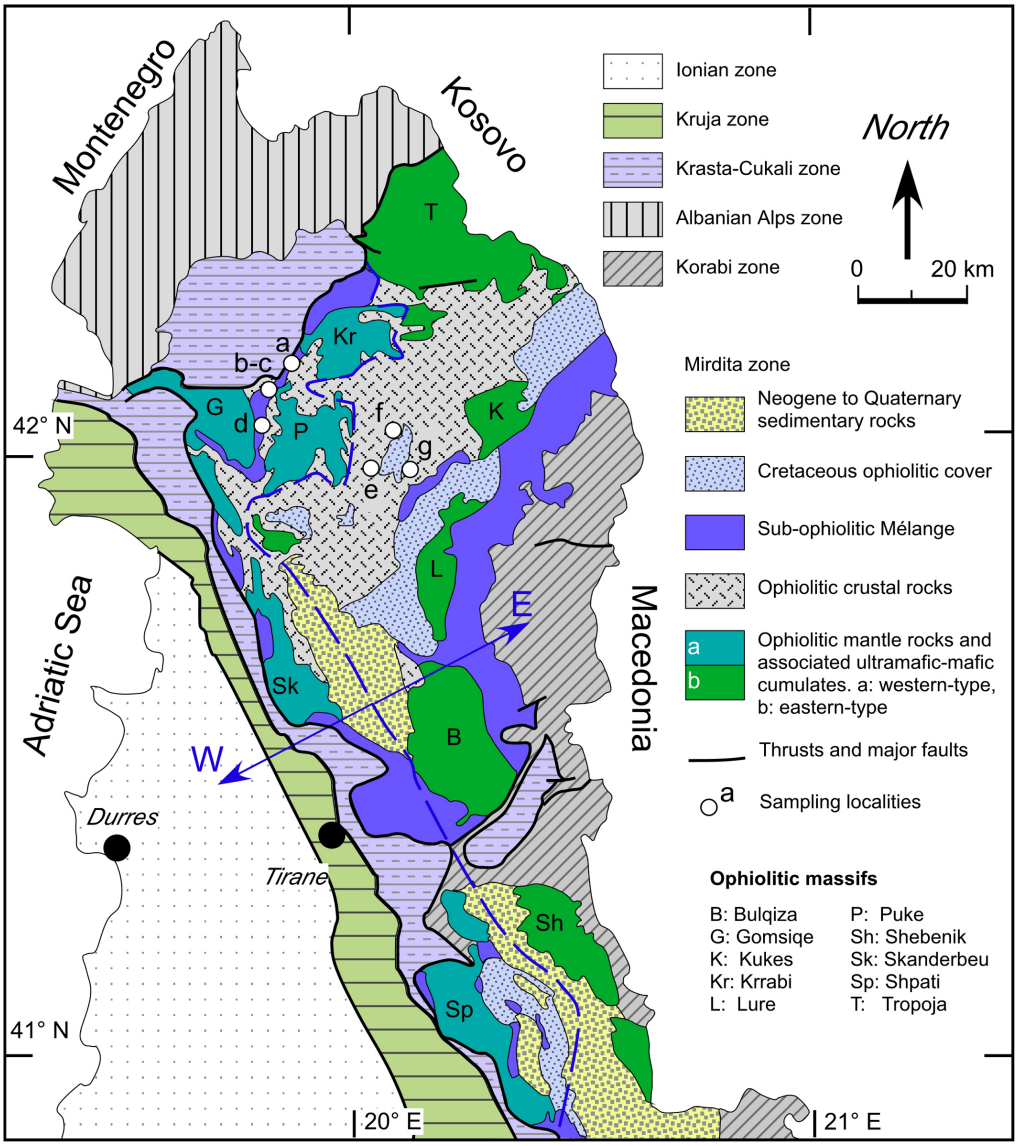

Fig. 2 - Simplified tectonic map of Central-Northern Albania (modified from Xhomo et al., 2002 and Hoeck et al., 2014) with the location of the sampled sections. The dashed line indicates the approximate boundary between the Western-type (W) and Eastern-type (E) ophiolites.

Rubik Complex, Bortolotti et al., 2013) with slices of metamorphic sole intercalated in-between. Interestingly, the same ophiolitic mélange (known as the Avdella Mélange, Pagondas Mélange, etc. in Greece and Ankara Mélange in Turkey) is found at the base of all the Hellenic-Turkish ophiolitic sequences, though many of these sequences are incomplete, being represented only by mantle peridotites (e.g., Photiades et al., 2003; Saccani and Photiades, 2005; Saccani et al., 2011, Chiari et al., 2012; Bortolotti et al., 2018). The sub-ophiolitic mélange consists of an assemblage of blocks and/or thrust sheets of mainly: 1) Triassic-Jurassic carbonate sequence; 2) serpentinized mantle peridotites; 3) Triassic basalts showing alkaline, enriched (E-) mid-ocean ridge basalt (MORB), and normal (N-) MORB compositions; 4) Jurassic basalts showing N-MORB, medium-Ti basalt (MTB), and boninitic compositions (Bortolotti et al., 1996; 2002; 2004; 2013; Saccani and Photiades, 2005). These features are also observed in the sub-ophiolitic mélange units in the many ophiolitic complexes of the Hellenides (e.g., Jones et al., 1992; Bortolotti et al., 2003, 2008; Chiari et al., 2012).

The WMO reconstructed stratigraphic sequence (Fig. 3a) includes, from bottom to top: 1) mantle tectonites largely consisting of lherzolites showing variable degree of depletion as a consequence of previous partial melting and melt extraction coupled with subsequent relative enrichment by subduction-derived fluids (see Saccani et al., 2011; Saccani et al., 2017); 2) a layered mafic-ultramafic cumulitic sequence; 3) a mafic to differentiated intrusive sequence; 4) a poorly developed sheeted dyke complex; 5) a volcanic sequence. The layered mafic-ultramafic cumulitic sequence is largely composed of typical MORB-type rocks, including dunites, plagioclase-dunites, troctolites, wehrlites, mela-gabbros, and gabbros (e.g., Saccani and Tassinari, 2015). Nonetheless, this sequence locally includes, especially in southern Albania, rock types that characteristically occur in SSZ type settings, such as websterites and orthopyroxenites, (Hoeck et al., 2002; 2014; Koller et al., 2006). The upper intrusive sequence is largely dominated by gabbros with very scarce Fe-gabbros, plagiogranites and gabbronorites (Beccaluva et al., 1994). The volcanic sequence includes pillow lava basalts showing high-Ti, N-MORB affinity alternate with MTBs formed in a nascent forearc setting (see Saccani et al., 2011; Saccani, 2015). These sequences are cross cut by boninitic dykes and locally topped by boninitic lava flows (Bortolotti et al., 1996; 2002, Bébien et al., 2000; Hoeck et al., 2002; Dilek and Furnes, 2008; Saccani et al., 2011; 2017).

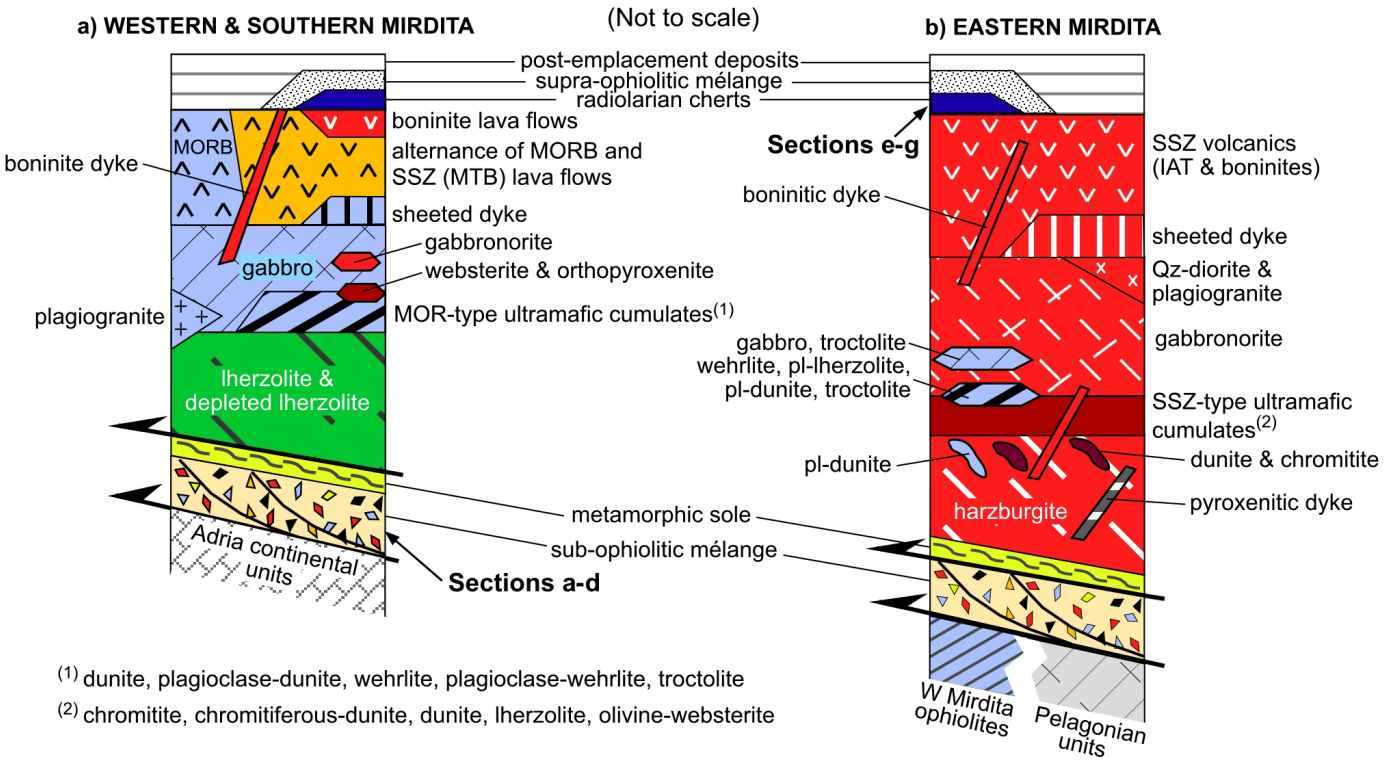

Fig. 3 - Reconstructed logs of the Western-type (a) and Eastern-type (b) Mirdita ophiolites. Compiled from: Beccaluva et al. (1994), Shallo (1994), Bébien et al. (2000), Bortolotti et al. (2002; 2013), Hoeck et al. (2002; 2014) and Saccani et al. (2011). The stratigraphic position of the sampled section is also shown. IAT: Island arc tholeiitic basalt; MORB: mid-ocean ridge basalt; MTB: medium-Ti basalt; SSZ: supra-subduction zone.

The reconstructed stratigraphic sequence of the EMO (Fig. 3b) includes (from bottom to top): 1) mantle tectonites exclusively represented by clinopyroxene-rich harzburgites, depleted harzburgites, and very depleted harzburgites (Saccani et al., 2017); 2) a layered mafic-ultramafic cumulitic sequence; 3) a mafic to differentiated intrusive sequence; 4) a thick sheeted dyke complex; 5) a volcanic sequence. Mantle harzburgites frequently show dunite and chromitite pods and lenses, whose abundance increases towards the upper part of the mantle section featuring a transition to the overlying ultramafic-mafic cumulates. Ultramafic cumulates consist of dunites with chromitite layers, olivine-websterites, and websterites (Saccani and Tassinari, 2015). Though the EMO show the typical complete ophiolitic sequence observed in SSZ ophiolites, layers of MOR-type rocks, such as plagioclase-lherzolites, troctolites, and gabbros occur in the cumulitic sequences of the Bulqiza and Shebenik ultramafic massifs (Beccaluva et al., 1994; Bébien et al., 1998), as well as in south Albania (Koller et al., 2006). Both cumulitic and isotropic mafic rocks are largely dominated by olivine-gabbronorites and gabbronorites and are followed upwards by abundant quartz-diorites and plagiogranites. The sheeted dike complex and the volcanic sequence include basalts, basaltic andesites, andesites, dacites and rhyolites showing both low-Ti, island arc tholeiitic (IAT) and very low-Ti boninitic affinities (Beccaluva et al., 1994; Shallo, 1994; Bortolotti et al., 1996; Bébien et al., 2000). Volcanic rocks occur as both massive and pillow lavas. Finally, the whole ophiolitic sequence is frequently cross cut by boninitic dykes.

Radiolarian cherts associated with WMO lavas gave latest Bajocian-early Bathonian to late Bathonian-early Callovian ages (UAZ 5 to UAZ 7) and late Bajocian/latest Bajocian-early Bathonian to middle Callovian-early Oxfordian (UAZ 4-5 to UAZ 8) for EMO lavas (Marcucci et al., 1994; Marcucci and Prela, 1996; Chiari et al. 1994; 2002; 2004; Prela et al., 2000). Both the WMO and EMO share the same post-emplacement deposits, which include the Late Jurassic-Early Cretaceous supra-ophiolitic mélange (Simoni Mélange) and Firza Flysch and the Early-Late Cretaceous post-orogenic carbonate sequence (Bortolotti et al., 2013).

The formation of the Dinaride-Hellenide Neo-Tethys is inferred to have started at the Early-Middle Triassic boundary, as testified by the age of radiolarian cherts stratigraphically associated with N-MORBs found in the sub-ophiolitic mélanges (Bortolotti et al., 2002; 2004; 2006). Mid-oceanic spreading in this Neo-Tethyan oceanic sector was then effective up to Middle Jurassic times, when the intra-oceanic subduction started (Dilek et al., 2005; 2008).

Saccani et al. (2011; 2017), and van Hinsbergen et al., (2020) suggested that the WMO and EMO collectively record the spatial and temporal variation of progressive mantle evolution and melt formation in the upper plate of a subducting slab from the very early stages of subduction initiation through a mature stage of an established subduction zone. In particular, the WMO record the Mid Jurassic inception of the intra-oceanic subduction characterized by the transition from mid-ocean ridge volcanic activity (N-MORB) to nascent forearc volcanism (MTB and boninites), whereas the EMO record a relatively mature subduction stage with production of IAT and boninitic magmatic rocks.

GEOCHEMICAL FEATURES OF THE JURASSIC VOLCANIC ROCKS

This section briefly resumes the geochemical features of the Jurassic ophiolitic volcanic rocks cropping out in both the WMO and EMO sequences, as well as those incorporated as blocks and tectonic slices within the sub-ophiolitic mélange units. In the lack of direct evidence from the volcanic rocks associated with the studied radiolarian cherts, this brief summary will be useful for discussing the significance of biostratigraphic ages obtained in this paper in the light of the magmatic and geodynamic evolution of the Mirdita Neo-Tethys during Middle Jurassic times. It should be noted that the sub-ophiolitic mélange units also include abundant Triassic volcanic rocks, which will not however be discussed here, as Triassic biostratigraphy and magmatism are beyond the scope of this paper. Research during the last decades on the geochemistry and petrogenesis of oceanic upper crustal rocks in the Jurassic ophiolites of the Albanides has led to the recognition of four different types of volcanic and subvolcanic rocks (e.g., Shallo, 1994; Beccaluva et al., 1994; 2005; Bortolotti et al., 1996; 2002; 2013; Bébien et al., 2000; Hoeck et al. 2002; Saccani et al., 2004; 2011; Saccani and Photiades, 2005; Dilek et al., 2005; 2007; 2008). They are: 1) high-Ti mid-ocean ridge basalts showing N-MORB compositions; 2) medium-Ti basalts (MTB); 3) low-Ti, island arc tholeiitic (IAT) basalts, basaltic andesites, andesites, and rhyolites; (4); very low-Ti boninitic basalts, basaltic andesites, andesites, and rhyolites.

High-Ti, normal-type mid ocean ridge basalts (High-Ti N-MORB)

Jurassic N-MORBs are found in both volcanic sequences of the WMO and in the sub-ophiolitic mélange (e.g., Bortolotti et al., 2002; Saccani and Photiades, 2005; Dilek et al., 2008; Monjoie et al., 2008). These rocks display a clear sub-alkaline affinity as exemplified by their low Nb/Y ratios (0.02-0.09). Their Ti/V ratios range from 26 to 39 (Fig. 4), clustering in the field of basalts generated at mid-ocean ridge settings (Shervais, 1982). Their overall geochemical features are similar to those of basalts generated at mid-ocean ridges. For example, relatively primitive basalts have TiO_2 = 0.76-2.23 wt%, P_2O_5 = 0.08-0.22 wt%, and V = 133-434 ppm values. No significant Th and Nb depletions or enrichments with respect other incompatible elements are observed in these basalts. Rare earth elements (REE) patterns of near-primitive basalts show depletion in light REE (LREE) with respect to medium REE (MREE) and heavy REE (HREE), as evidenced by the La_N/Sm_N (0.41-0.78) and La_N/Yb_N (0.34-0.86) ratios. All data are from Saccani et al. (2011; 2017). Plotted in the Th-Nb diagram in Fig. 5a, the Jurassic N-MORBs do not show any detectable subduction influence and cluster in the field for typical N-MORB compositions.

The low Zr/Y ratios (< 4) and very low Ta/Yb ratios (< 0.08) indicate that these rocks likely originated from partial melting of a depleted N-MORB type sub-oceanic mantle source, with no influence of enriched ocean island basalt (OIB) components. In fact, Saccani et al. (2011; 2017) using REE modelling have demonstrated that near-primitive N-MORBs are generally compatible with 10-20% partial melting of a depleted MORB mantle (DMM) source (Workman and Hart, 2005).

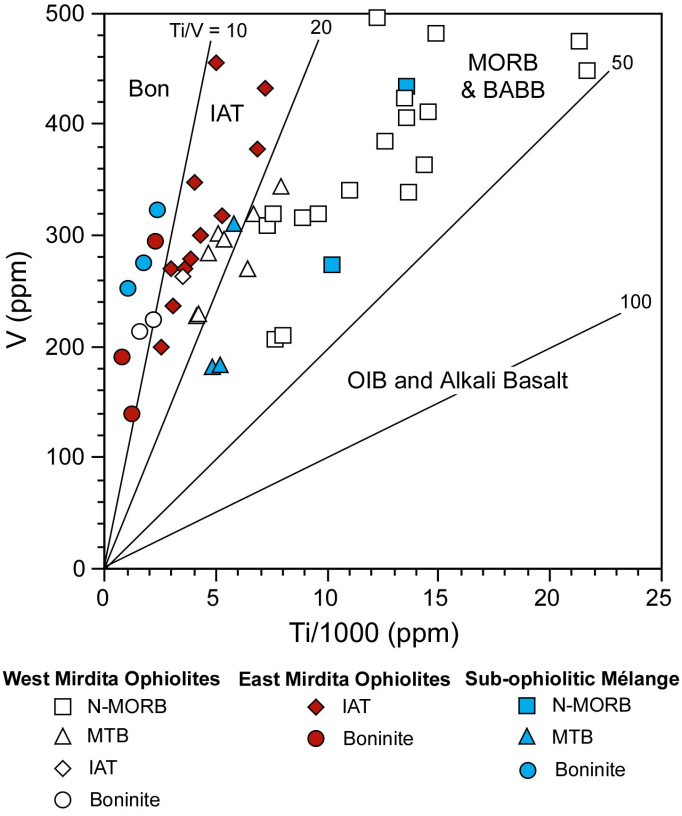

Fig. 4 - V vs. Ti/1000. Tectonic discrimination diagrams (Shervais, 1982) for the Jurassic basalts from the Mirdita ophiolites and Sub-ophiolitic Mélange. Data from: Bortolotti et al. (2002), Hoeck et al. (2002), Saccani et al. (2004), Saccani and Photiades (2005), Dilek et al. (2008) and Monjoie et al. (2008). Abbreviations: BABB: backarc basin basalt; Bon: Boninite; IAT: Island arc tholeiitic basalt (low-Ti basalt); MTB: medium-Ti basalt; N-MORB: normal-type mid-ocean ridge basalt (high-Ti basalt); OIB: ocean island basalt.

Medium-Ti basalts (MTB)

MTBs crop out in the WMO of the northern Albanides, in the southern Albanides, and as blocks included in the sub-ophiolitic mélange (Bortolotti et al., 2002; Hoeck et al., 2002; Saccani and Photiades, 2005). These basalts show geochemical characteristics that are intermediate between those of N-MORBs and IATs (Bébien et al., 2000; Saccani et al., 2011; Saccani, 2015). Compared to N-MORB, they show slightly lower contents in TiO_2 (0.67-1.09 wt%), P_2O_5 (0.01-0.17 wt%), Zr (5-90 ppm), and Y(18-29 ppm). Their Ti/V ratios (16-28) straddle the boundary between the IAT and MORB fields (Fig. 4). The contents of high field strength elements (HFSE) are slightly lower than those of N-MORBs with comparable degrees of fractionation, but Th, Ta, and Nb concentrations are highly depleted with respect to those of N-MORBs. Their Th and Nb values are about 0.1 times N-MORB composition and are also significantly lower than those of IAT and boninitic basalts, (Saccani et al., 2011; 2017). MREE, and HREE compositions are slightly lower than those of N-MORBs, but LREE concentrations are highly depleted with respect to those of N-MORBs (Saccani et al., 2011; 2017). In fact, La_N/Yb_N ratios are in the range of 0.01-0.25. Accordingly, they display no Th enrichment with respect to Nb, indicating no detectable subduction-related contribution (Bortolotti et al., 2002; Saccani, 2015). In Fig. 5a, MTBs plot in the field for nascent forearc basalts. Saccani et al. (2011; 2017) have suggested that primary MTB

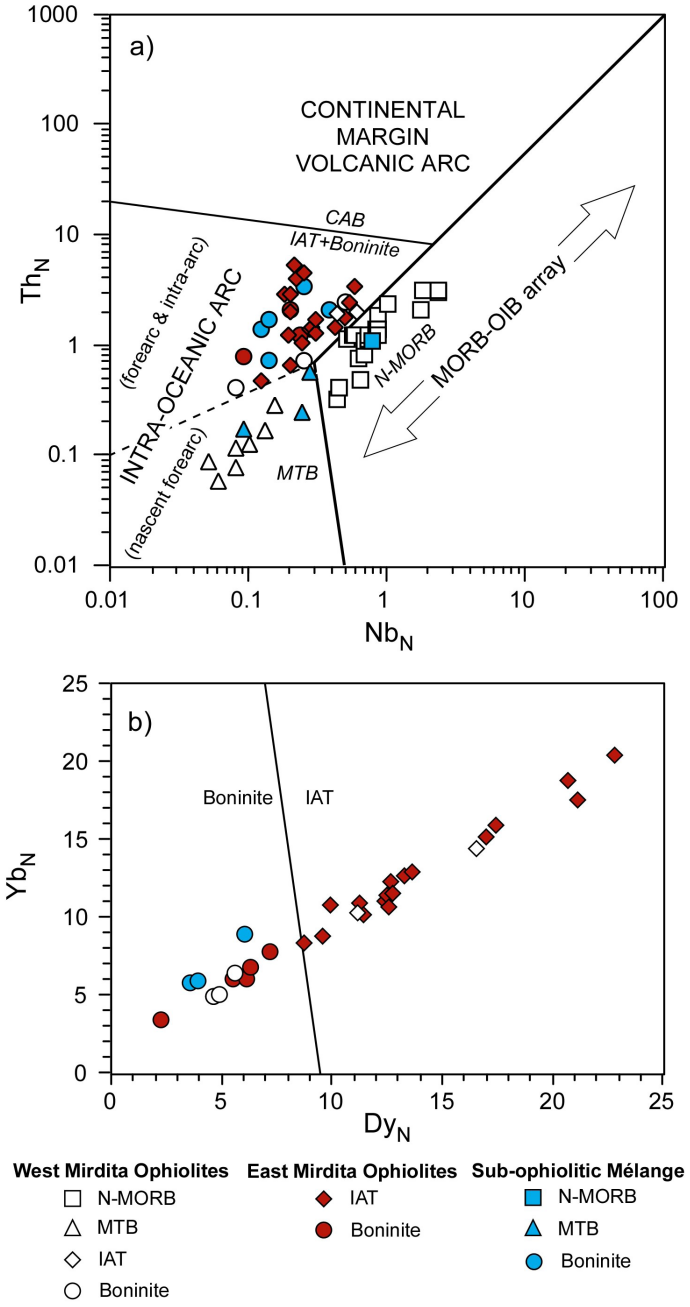

Fig. 5 - a) N-MORB normalized Th vs. Nb and b) chondrite-normalized Yb vs. Dy tectonic discrimination diagrams (Saccani, 2015) for the Jurassic basalts from the Mirdita ophiolites and Sub-ophiolitic Mélange. Data from: Bortolotti et al. (2002), Hoeck et al. (2002), Saccani et al (2004), Saccani and Photiades (2005), Dilek et al. (2008) and Monjoie et al. (2008). Normalizing values are from Sun and McDonough (1989). Abbreviations: CAB: calc-alkaline basalt; IAT: Island arc tholeiitic basalt (low-Ti basalt); MTB: medium-Ti basalt; N-MORB: normal-type mid-ocean ridge basalt (high-Ti basalt); OIB: ocean island basalt.

melts originated low degrees of partial melting (~ 5-8 %) of depleted lherzolites left as the residual mantle after the initial N-MORB melt extraction without any detectable LREE and Th enrichment by subduction-related fluids.

Low-Ti island arc tholeiitic rocks (IAT)

This rock-group exclusively crops out in the EMO (e.g., Beccaluva et al., 1994; Dilek et al., 2008; Saccani et al., 2011). These rocks are mainly represented by fractionated products, such as basaltic andesites, andesites, and dacites, whereas near-primitive IAT basalts are rare. Basaltic rocks have relatively low TiO_2 contents (0.48-1.10 wt%) and low Ti/V ratios (Fig. 4). They also have relatively low contents of P_2O_5 (0.04-0.06 wt%). N-MORB normalized incompatible elements exhibit depleted patterns compared to N-MORB compositions, and display mild negative anomalies in Th, Ta, and Nb (Saccani et al., 2011). These rocks are characterized by depletion in LREE, as exemplified by low La_N/Yb_N (0.20-0.63) ratios. They show a clear Th enrichment with respect to Nb, suggesting some influence of subduction-derived components (Fig. 5a). In Fig, 5b, these rocks plot in the field for IAT basalts (Saccani, 2015).

The chemistry of near-primitive IAT basalts is consistent with an origin from partial melting of refractory mantle sources. Their Th enrichment relative to Nb suggests an arc signature (Dilek et al., 2008; Saccani et al., 2011; 2017; Saccani, 2015) showed that REE patterns of the near-primitive IAT basalts are consistent with ~ 10-20% partial melting of residual MORB mantle lherzolites, which were slightly enriched in LREE by subduction-derived fluids.

Very low-Ti boninitic rocks

Very low-Ti, boninitic rocks mainly crop out in the EMO sequences, but are also fairly abundant in the WMO, where they occur as both lava flows and dykes (Bortolotti et al., 2002; Dilek et al., 2008). Moreover, they are largely represented in the sub-ophiolitic mélange (Saccani et al., 2005). Boninitic basalts are characterized by very low TiO_2 contents (0.12-0.46 wt%) and Ti/V ratios (Fig. 4), which are comparable with those of typical boninitic rocks from forearc regions of oceanic island arcs (e.g., Crawford et al., 1989; Pearce et al., 1992). Accordingly, their P_2O_5 (< 0.10 wt%), Zr (< 6 ppm) and Y (< 11 ppm) contents are very low. Compatible element contents, such as Ni (up to 869 ppm) and Cr (up to 1739 ppm), are also very high. Very low-Ti boninitic basalts are strongly depleted in HFSE but Th (Saccani et al., 2011). Commonly, they display U-shaped REE patterns typical of boninites, with La_N/Sm_N = 1.03-2.85 and Sm_N/Yb_N = 0.25-0.78. Similar to IAT basalts, they show a clear Th enrichment with respect to Nb, suggesting subducted slab influence (Fig. 5a), whereas in the classification diagram in Fig. 5b, they plot in the field for boninitic basalts.

Saccani et al. (2011; 2017) suggested that primary boninite melts may have been generated by high degrees of partial melting (15-25%) of a refractory harzburgitic source, which is residual after the extraction of MTB and/or IAT primary melts but significantly enriched in LREE.

THE SAMPLED SECTIONS

Sampling was focused on the radiolarian cherts deposited in the upper part of the ophiolitic volcanic series in northern Albania. Samples were taken in seven sections in northern Albania (Fig. 2). In the WMO, four sections were focused on the radiolarian cherts included in the sub-ophiolitic mélange (Fig. 3a). They are: a) Koman; b) Karma 1; c) Karma 2; d) Gomsique. In the EMO, three sections were focused on the radiolarian cherts forming the sedimentary cover of the ophiolitic unit (Fig. 3b). They are: e) Gurth; f) Gurth 2; g) Gurth 4.

a) Koman. This section is located near the mining galleries of Palaj near the Koman dam (N 42^0 05′ 03″, E 19^0 48′

31″). It consists of very altered basalts which include 1.30 m of red radiolarian cherts. The chert sample AL374 was collected near the lower contact with the basalt.

b) Karma 1. This section is located along the road from Koman to Karma (N 42^0 05′ 06″, E 19^0 48′ 36″). It consists of almost totally altered basalts with a level of 1.5 m of red radiolarian cherts, the chert sample AL371 was collected about 0.5 m from the lower contact with the basalt.

c) Karma 2. This section is located about 150 m from Karma 1 and consist of very altered volcanic rocks, most likely represented by pillow basalts with a level of 3 m of red radiolarian cherts where the sample AL372 was collected.

d) Gomsique. This sampling area is located near the road to Vau Dejës village about 1 km from the Gomsique bridge (N 42^0 01′ 21″, E 19^0 40′ 03″). In this area, cherts were found in two distinct outcrops. The first one consists of about 40 m of altered basalts with chert layers in between. Sample AL1205 was collected in a red radiolarian chert of about 20 cm. The second one consists of a thin sedimentary sequence including limestones, pelagic mudstones, and radiolarian cherts. Sample AL1205b was taken in a chert level of about 0.3 m close to the mudstone beds.

e) Gurth. This section is located about 500 m from Gurth mine (N 41^0 55′ 34″, E 20^0 04′ 05″). It consists of very altered intermediate to acidic volcanic rocks (most likely andesites) with a level of red radiolarian cherts of about 2 m. Two chert samples, GU7 and GU8, were collected in this section about 0.4 and 1.5 m from the lower contact with the volcanic rocks.

f) Gurth 2. This section is located about 6 km NE from the Gurth Spaç village and it consists of about 4.9 meters of red cherts and shales, greenish-gray cherts and red cherts. The supra-ophiolitic mélange (Simoni Mélange) unconformably covers the cherts. Three chert samples were collected: G2-1 at 20 cm from the base of the cherts, G2-3 at 0.45 cm from the base, and the last sample G2-2 at 0.90 m from the base.

g) Gurth 4. This section is located NE from the Gurth Spaç village (N 41^0 55′ 43″, E 20^0 03′ 43″) and consists of about 2.5 m of red radiolarian cherts in contact with altered andesitic/dacitic lava flows. Two samples were taken for radiolarian analyses G4-1 and G4-3, respectively at 0.5 and 2 m above the andesites/dacites. The radiolarian cherts are unconformably covered by the supra-ophiolitic mélange (Simoni Mélange).

Radiolarian analyses

The twelve samples of radiolarian cherts have been etched with hydrofluoric acid at different concentrations. The samples yielded radiolarians with moderate-good preservation (Figs. 6-8). We utilized the radiolarian zonation based on Unitary Association zones (UAZ) proposed by Baumgartner et al. (1995) for the Middle Jurassic-Early Cretaceous (Aalenian-early Aptian interval) and for the taxonomy of radiolarian genera we followed O'Dogherty et al. (2006; 2009; 2017). In the following paragraphs we discuss the range of some taxa that were reported with a different age range in Baumgartner et al. (1995). The principal radiolarian markers are illustrated in Figs. 6-8.

Eoxitus hungaricus Kozur (= *Tethysetta dhimenaensis* ssp. A; UAZ 3-8 in Baumgartner et al., 1995) occurs also in the Carpathian up to the Tithonian (Paulian Dumitrica, pers. comm., as reported in Chiari et al., 2008). We could indicate a broader range for this taxon: UAZ 3-11 (early-middle Bajocian to late Kimmeridgian-early Tithonian).

Eucyrtidiellum dentatum Baumgartner (= *Eucyrtidiellum unumanese dentatum*; UAZ 6-7 in Baumgartner et al., 1995). Šegvić et al. (2014) found this taxon in a sample of UAZ 5 age (latest Bajocian-early Bathonian), therefore the range of *E. dentatum* could be indicated as UAZ 5-7 (latest Bajocian-early Bathonian to late Bathonian-early Callovian).

Eucyrtidiellum pustulatum Baumgartner. Baumgartner et al. (1995) indicated an UAZ 5-8 range (latest Bajocian-early Bathonian to middle Callovian-early Oxfordian) while Gawlick et al. (2016) indicated a broader range.

Kilinora (?) *oblongula* (Kocher) (= *Stylocapsa oblongula*; UAZ 6-8 in Baumgartner et al., 1995). The range of this taxon could be UAZ 5-8 (latest Bajocian-early Bathonian to middle Callovian-early Oxfordian). In fact Gawlick et al. (2016) found *K.* (?) *oblongula* in the sample AL 1993 of UAZ 5 age (latest Bajocian-early Bathonian).

Hexasaturnalis nakasekoi Dumitrica and Dumitrica-Jud (= *Acanthocircus suboblongus suboblongus*; UAZ 3-11 in Baumgartner et al., 1995 only Fig. 1). This taxon, one of the most common saturnalid, was described for the first time by Dumitrica and Dumitrica-Jud (2005) and its range is referable to the interval Bathonian-late Kimmeridgian/early Tithonian (Dumitrica and Dumitrica-Jud, 2005).

Hexasaturnalis suboblongus (Yao) (= *Acanthocircus suboblongus suboblongus*; UAZ 3-11 in Baumgartner et al., 1995). After Dumitrica and Dumitrica-Jud (2005) the range of this taxon is early-middle Bajocian to late Bajocian (UAZ 3-4) after Chiari et al. (2007) the range of this taxon could be longer: early-middle Bajocian to latest Bajocian-early Bathonian (UAZ 3-5). Furthermore Carter et al. (2010) reported the first appearance of this taxon in the late Aalenian (UA 39) *Mirifusus proavus-Transhsuum hisuikyoense* Zone, this zone is in good agreement with UAZ 2. Taking into consideration these correlations we could assign to *Hexasaturnalis suboblongus* an UAZ 2-5 range (late Aalenian to latest Bajocian-early Bathonian).

Striatojaponocapsa synconexa O'Dogherty, Goričan and Dumitrica (= *Tricolocapsa plicarum* ssp. A; UAZ 4-5 in Baumgartner et al., 1995). Prela et al. (2000) indicated for this taxon a longer range: late Bajocian to middle Bathonian (UAZ 4-6?), O'Dogherty et al. (2006) found this taxon in samples (VS3, VS4) of middle Bathonian age (UAZ 6) while Matsuoka and Ito (2019) indicated the last occurrence of *S. synconexa* in the lower part of *Striatojaponocapsa conexa* Zone (late Bathonian). We could assign to *Striatojaponocapsa synconexa* an age range from late Bajocian to late Bathonian.

Theocapsommella cucurbiformis (Baumgartner) (= *Theocapsomma cucurbiformis*; UAZ 6-7 in Baumgartner et al., 1995). The range of this taxon could be considered longer UAZ 5-7 (latest Bajocian-early Bathonian to late Bathonian-early Callovian) because Halamic et al. (1999) and Prela et al. (2000) found this taxon in samples of UAZ 5 (latest Bajocian-early Bathonian).

Unuma gordus Hull (= *Unuma* sp. A; UAZ 4-6 in Baumgartner et al., 1995). After Auer et al. (2009) this taxon could reach also the middle/late Oxfordian boundary or the late Oxfordian.

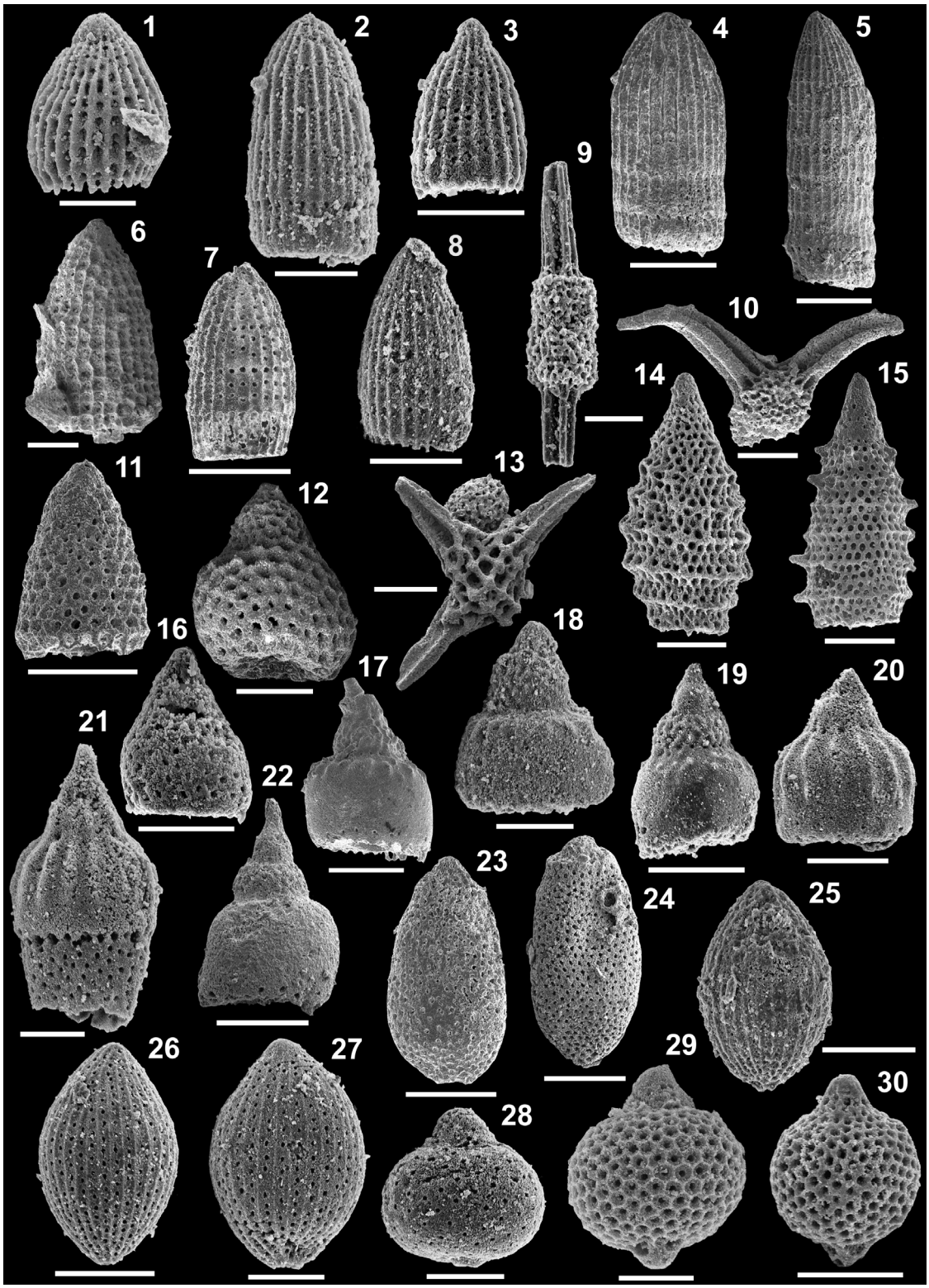

Fig. 6 - (scale bar = 50μm). 1) *Archaeodictyomitra publica* (Hull), GU8; 2) *Archaeodictyomitra exigua* Blome, GU8; 3) *Archaeodictyomitra patricki* Kocher, AL372; 4) *Archaeodictyomitra praeapiarium* Cordey, AL1205b; 5) *Archaeodictyomitra prisca* Kozur and Mostler, AL1205b; 6) *Archaeodictyomitra* sp. cf. *A. cellulata* O'Dogherty, Goričan and Dumitrica, AL1205b; 7) *Archaeodictyomitra* sp. cf. *A. exigua* Blome, AL1205b; 8) *Archaeodictyomitra* sp. cf. *A. rigida* Pessagno, G4-1; 9) *Archaeospongoprunum elegans* Wu AL372; 10) *Bernoullius cristatus* Baumgartner, AL372; 11) *Campanomitra ulivii* (Chiari, Marcucci and Prela), AL1205b; 12) *Doliocapsa magnipora* (Chiari, Marcucci and Prela), AL1205; 13) *Emiluvia premyogii* Baumgartner, AL372; 14) *Eoxitus baloghi* Kozur, AL372; 15) *Eoxitus hungaricus* Kozur, AL1205b; 16) *Eucyrtidiellum* (?) *circumperforatum* Chiari, Cortese and Marcucci, AL372; 17) *Eucyrtidiellum dentatum* Baumgartner, AL1205b; 18) *Eucyrtidiellum dentatum* Baumgartner, G2-1; 19) *Eucyrtidiellum pustulatum* Baumgartner, G4-1; 20) *Eucyrtidiellum semifactum* Nagai and Mizutani, G4-3; 21) *Eucyrtidiellum semifactum* Nagai and Mizutani, GU8; 22) *Eucyrtidiellum unumaense* (Yao), AL372; 23) *Guexella nudata* (Kocher), AL1205b; 24) *Guexella nudata* (Kocher), AL372; 25) *Helvetocapsa matsuokai* (Sashida), AL372; 26) *Helvetocapsa matsuokai* (Sashida), G4-1; 27) *Helvetocapsa matsuokai* (Sashida), GU8; 28) *Hemicryptocapsa buekkense* (Kozur), GU7; 29) *Hemicryptocapsa marcucciae* (Cortese), GU8; 30) *Hemicryptocapsa marcucciae* (Cortese), G2-2.

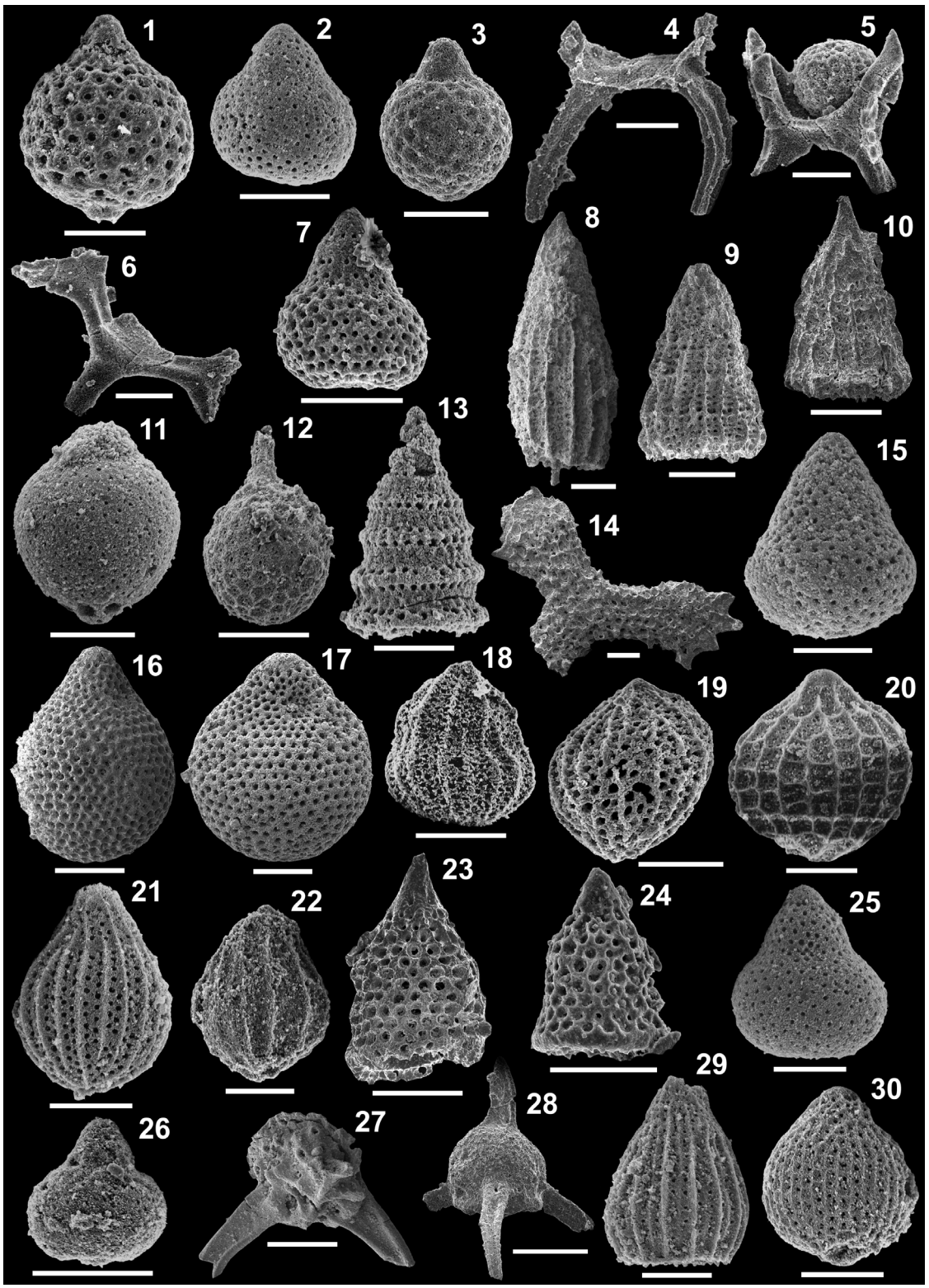

Fig. 7 - (scale bar = 50 μm). 1) *Hemicryptocapsa yaoi* (Kozur), GU7; 2) *Hemicryptocapsa* sp. cf. *H. buekkense* (Kozur), G4-3; 3) *Hemicryptocapsa* sp. cf. *H. yaoi* (Kozur), AL372; 4) *Hexasaturnalis nakasekoi* Dumitrica and Dumitrica-Jud, AL 372; 5) *Hexasaturnalis suboblongus* (Yao), AL372; 6) *Hexasaturnalis* sp. cf. *H. tetraspinus* (Yao), AL372; 7) *Hiscocapsa kodrai* (Chiari, Marcucci and Prela), AL1205; 8) *Hsuum matsuokai* Isozaki and Matsuda, AL1205b; 9) *Hsuum* sp. cf. *H. belliatulum* Pessagno and Whalen, AL1205b; 10) *Hsuum* sp. cf. *H. mirabundum* Pessagno and Whalen, AL1205b; 11) *Japonocapsa* sp. aff. *J. fusiformis* (Yao) sensu Matsuoka (1983), GU7; 12) *Kilinora* (?) *oblongula* (Kocher), AL372; 13) *Mizukidella kamoensis* (Mizutani and Kido), AL372; 14) *Paronaella bronnimanni* Pessagno, AL 1205b; 15) *Praewilliriedellum convexum* (Yao), GU 7; 16) *Praewilliriedellum robustum* (Matsuoka), AL1205b; 17) *Praewilliriedellum robustum* (Matsuoka), AL372; 18) *Protunuma lanosus* Ozvoldova, AL 372; 19) *Protunuma ochiensis* Matsuoka, AL1205; 20) *Protunuma quadriperforatus* O'Dogherty and Goričan, AL1205b; 21) *Protunuma turbo* Matsuoka, GU 8; 22) *Protunuma* sp. cf. *P. lanosus* Ozvoldova, G2-1; 23) *Pseudodictyomitrella renevieri* O'Dogherty, Goričan and Dumitrica, AL 1205b; 24) *Pseudodictyomitrella* sp. aff. *P. cappa* (Cortese), AL1205; 25) *Quarkus japonicus* (Yao), GU7; 26) *Quarkus* sp. cf. *Q. madstonense* (Pessagno, Blome and Hull), G2-1; 27) *Saitoum pagei* De Wever, AL1205b; 28) *Saitoum* sp. cf. *S. levium* De Wever, AL1205b; 29) *Semihsuum amabile* (Aita), GU8; 30) *Striatojaponocapsa conexa* (Matsuoka), G2-3.

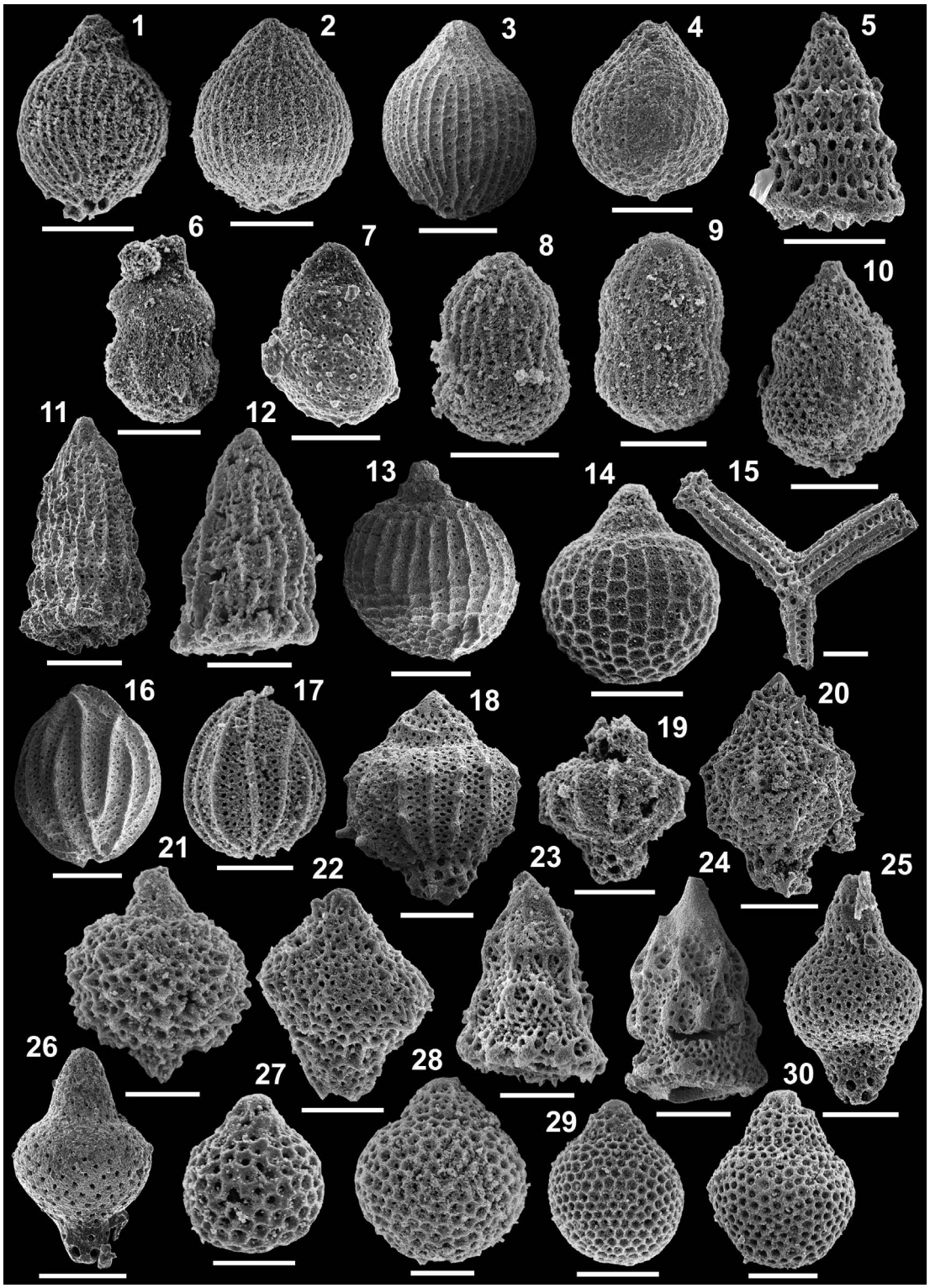

Fig. 8 - (scale bar = 50µm). 1) *Striatojaponocapsa plicarum* (Yao), AL372; 2) *Striatojaponocapsa synconexa* O'Dogherty, Goričan and Dumitrica, AL372; 3) *Striatojaponocapsa synconexa* O'Dogherty, Goričan and Dumitrica, AL1205b; 4) *Striatojaponocapsa* sp. cf. *S. synconexa* O'Dogherty, Goričan and Dumitrica, G2-2; 5) *Takemuraella* sp. cf. *T. schardti* O'Dogherty, Goričan and Dumitrica, AL372; 6) *Theocapsommella cucurbiformis* (Baumgartner), G2-1; 7) *Theocapsommella himedaruma* (Aita), AL1205; 8) *Theocapsommella medvednicensis* (Goričan), AL37; 9) *Theocapsommella medvednicensis* (Goričan), G2-1; 10) *Theocapsommella* sp. cf. *T. cucurbiformis* (Baumgartner), AL372; 11) *Transhsuum parasolense* (Pessagno and Whalen), AL1205; 12) *Transhsuum* sp., G2-2; 13) "*Tricolocapsa*" *tetragona* Matsuoka, AL1205b; 14) "*Tricolocapsa*" *tetragona* Matsuoka, G4-3; 15) *Tritrabs* sp. cf. *T. rhododactylus* Baumgartner, AL1205; 16) *Unuma gordus* Hull, AL1205b; 17) *Unuma gordus* Hull, G2-2; 18) *Unuma latusicostatus* (Aita), AL1205b; 19) *Unuma latusicostatus* (Aita), G4-3; 20) *Unuma* sp. aff. *U. latusicostatus* (Aita), AL1205b; 21) *Williriedellum formosum* (Chiari, Marcucci and Prela), GU8; 22) *Williriedellum nodosum* Chiari, Marcucci and Prela, AL372; 23) *Xitus skenderbegi* (Chiari, Marcucci and Prela), AL372; 24) *Xitus skenderbegi* (Chiari, Marcucci and Prela), AL1205b; 25) *Yaocapsa* sp. aff. *Y. mastoidea* (Yao) sensu Goričan et al. (2012), AL372; 26) *Yaocapsa* sp. aff. *Y. mastoidea* (Yao) sensu Goričan et al. (2012), AL1205b; 27) *Zhamoidellum* sp. 2 sensu O'Dogherty et al. (2006), G2-2; 28) *Zhamoidellum* sp. aff. *Z. ventricosum* Dumitrica, GU8; 29) *Zhamoidellum* sp. aff. *Z. ventricosum* Dumitrica, G4-3; 30) *Zhamoidellum* sp., AL372.

Zhamoidellum ventricosum Dumitrica (UAZ 8-11; in Baumgartner et al., 1995). Several authors indicated a broader range for this taxon (Šmuc and Goričan, 2005; O'Dogherty et al., 2006; Danelian et al., 2008 and Gawlick et al., 2018). Šmuc and Goričan (2005) found this taxon in a sample (M8 21,90) of UAZ 6-7 age (middle Bathonian to late Bathonian-early Callovian) while Gawlick et al. (2018) found *Z. ventricosum* in the sample SRB 262 of probably Bathonian age, thererefore taking into in consideration these data we could indicate an UAZ 6 to UAZ 11 range for this taxon (middle Bathonian to late Kimmeridgian-early Tithonian).

The radiolarian assemblages and the ages in the examined samples are the following:

Sub-ophiolitic mélange (Rubik Complex)

a) Koman

AL374: *Striatojaponocapsa synconexa* O'Dogherty, Goričan and Dumitrica, *Theocapsommella medvednicensis* (Goričan), *Unuma gordus* Hull, *Zhamoidellum* sp.

Age: late Bajocian to late Bathonian-early Callovian **(UAZ 4-7)** for the occurrence of *Unuma gordus* Hull and *Striatojaponocapsa synconexa* O'Dogherty, Goričan and Dumitrica.

b) Karma 1

AL371: *Striatojaponocapsa plicarum* (Yao), *Striatojaponocapsa synconexa* O'Dogherty, Goričan and Dumitrica, *Theocapsommella* sp. cf. *T. cordis* (Kocher).

Age: late Bajocian to latest Bajocian-early Bathonian (UAZ 4-5) for the presence of *Striatojaponocapsa synconexa* O'Dogherty, Goričan and Dumitrica and *Striatojaponocapsa plicarum* (Yao).

c) Karma 2

AL372: *Archaeodictyomitra patricki* Kocher, *Archaeospongoprunum elegans* Wu, *Bernoullius cristatus* Baumgartner, *Doliocapsa magnipora* (Chiari, Cortese and Marcucci), *Emiluvia premyogii* Baumgartner, *Eoxitus baloghi* Kozur, *Eoxitus hungaricus* Kozur, *Eucyrtidiellum* (?) *circumperforatum* Chiari, Cortese and Marcucci, *Eucyrtidiellum dentatum* Baumgartner, *Eucyrtidiellum unumaense* (Yao), *Guexella nudata* (Kocher), *Helvetocapsa matsuokai* (Sashida), *Hemicryptocapsa yaoi* (Kozur), *Hemicryptocapsa* sp. cf. *H. yaoi* (Kozur), *Hexasaturnalis nakasekoi* Dumitrica and Dumitrica-Jud, *Hexasaturnalis suboblongus* (Yao), *Hexasaturnalis* sp. cf. *H. tetraspinus* (Yao), *Kilinora* (?) *oblongula* (Kocher), *Mizukidella kamoensis* (Mizutani and Kido), *Praewilliriedellum robustum* (Matsuoka), *Protunuma lanosus* Ozvoldova, *Quarkus japonicus* (Yao), *Semihsuum amabile* (Aita), *Striatojaponocapsa plicarum* (Yao), *Striatojaponocapsa synconexa* O'Dogherty, Goričan and Dumitrica, *Takemuraella* sp. cf. *T. schardti* O'Dogherty, Goričan and Dumitrica, *Theocapsommella* sp. cf. *T. cucurbiformis* (Baumgartner), *Tritrabs casmaliaensis* (Pessagno), *Unuma gordus* Hull, *Williriedellum nodosum* Chiari, Marcucci and Prela, *Xitus skenderbegi* (Chiari, Marcucci and Prela), *Yaocapsa* sp. aff. *Y. mastoidea* (Yao) sensu Goričan et al. (2012), *Zhamoidellum* sp.

Age: latest Bajocian-early Bathonian (UAZ 5) for the presence of *Bernoullius cristatus* Baumgartner, *Eucyrtidiellum dentatum* Baumgartner, *Guexella nudata* (Kocher), *Hexasaturnalis suboblongus* (Yao), *Praewilliriedellum robustum* (Matsuoka), *Yaocapsa* sp. aff. *Y. mastoidea* (Yao) sensu Goričan et al. (2012) and *Kilinora* (?) *oblongula* (Kocher) with *Striatojaponocapsa plicarum* (Yao). It is worth of note that in this sample is also present a specimen of *Hexasaturnalis nakasekoi* Dumitrica and Dumitrica-Jud, a taxon which is not included in the database of the zonation of Baumgartner et al. (1995). Anyway considering the range of this taxon, Bathonian-late Kimmeridgian/early Tithonian, the age of the sample AL 372 could be indicated as early Bathonian.

d) Gomsique

AL1205: *Doliocapsa magnipora* (Chiari, Marcucci and Prela), *Eucyrtidiellum dentatum* Baumgartner, *Hemicryptocapsa marcucciae* (Cortese), *Hemicryptocapsa yaoi* (Kozur), *Hiscocapsa kodrai* (Chiari, Marcucci and Prela), *Protunuma lanosus* Ozvoldova, *Protunuma ochiensis* Matsuoka, *Pseudodictyomitrella* sp. aff. *P. cappa* (Cortese), *Theocapsommella himedaruma* (Aita), *Transhsuum parasolense* (Pessagno and Whalen), *Tritrabs* sp. cf *T. rhododactylus* Baumgartner, *Unuma gordus* Hull, *Williriedellum formosum* (Chiari, Marcucci and Prela).

Age: latest Bajocian-early Bathonian to late Bathonian-early Callovian (UAZ 5-7) for the occurence of *Protunuma ochiensis* Matsuoka with *Eucyrtidiellum dentatum* Baumgartner.

AL1205b: *Archaeodictyomitra praeapiarium* Cordey, *Archaeodictyomitra prisca* Kozur and Mostler, *Archaeodictyomitra* sp. cf. *A. cellulata* O'Dogherty, Goričan and Dumitrica, *Archaeodictyomitra* sp. cf. *A. exigua* Blome, *Campanomitra ulivii* (Chiari, Marcucci and Prela), *Eoxitus hungaricus* Kozur, *Eucyrtidiellum dentatum* Baumgartner, *Guexella nudata* (Kocher), *Helvetocapsa matsuokai* (Sashida), *Hexasaturnalis* sp. cf. *H. nakasekoi* Dumitrica and Dumitrica-Jud, *Hsuum matsuokai* Isozaki and Matsuda, *Hsuum* sp. cf. *H. belliatulum* Pessagno and Whalen, *Hsuum* sp. cf. *H. mirabundum* Pessagno and Whalen, *Mizukidella kamoensis* (Mizutani and Kido), *Paronaella bronnimanni* Pessagno, *Praewilliriedellum convexum* (Yao), *Praewilliriedellum robustum* (Matsuoka), *Protunuma quadriperforatus* O'Dogherty and Goričan, *Pseudodictyomitrella renevieri* O'Dogherty, Goričan and Dumitrica, *Saitoum pagei* De Wever, *Saitoum* sp. cf. *S. levium* De Wever, *Semihsuum amabile* (Aita), *Striatojaponocapsa synconexa* O'Dogherty, Goričan and Dumitrica, *Transhsuum maxwelli* gr. (Pessagno) "*Tricolocapsa*" *tetragona* Matsuoka, *Unuma gordus* Hull, *Unuma latusicostatus* (Aita), *Unuma* sp. aff. *U. latusicostatus* (Aita), *Yaocapsa* sp. aff. *Y. mastoidea* (Yao) sensu Goričan et al. (2012), *Xitus skenderbegi* (Chiari, Marcucci and Prela), *Xitus* sp. cf. *X. skenderbegi* (Chiari, Marcucci and Prela), *Zhamoidellum* sp.

Age: latest Bajocian-early Bathonian (UAZ 5) for the occurrence of *Eucyrtidiellum dentatum* Baumgartner, *Guexella nudata* (Kocher), *Praewilliriedellum robustum* (Matsuoka), "*Tricolocapsa*" *tetragona* Matsuoka, *Yaocapsa* sp. aff. *Y. mastoidea* (Yao) sensu Goričan et al. (2012) with *Helvetocapsa matsuokai* (Sashida) and *Unuma latusicostatus* (Aita).

Eastern Mirdita Ophiolite (EMO)

e) Gurth

GU7: *Eucyrtidiellum semifactum* Nagai and Mizutani, *Hemicryptocapsa buekkense* (Kozur), *Hemicryptocapsa yaoi* (Kozur), *Hemicryptocapsa* sp. aff. *H. buekkense* (Kozur), *Japonocapsa* sp. aff. *J. fusiformis* (Yao) sensu Matsuoka (1983), *Praewilliriedellum convexum* (Yao), *Quarkus japonicus* (Yao), *Unuma gordus* Hull.

Age: latest Bajocian-early Bathonian to middle Bathonian (UAZ 5-6) for the occurrence of *Eucyrtidiellum semifactum* Nagai and Mizutani with *Japonocapsa* sp. aff. *J. fusiformis* (Yao) sensu Matsuoka (1983).

GU8: *Archaeodictyomitra publica* (Hull), *Archaeodictyomitra exigua* Blome, *Eucyrtidiellum semifactum* Nagai and Mizutani, *Helvetocapsa matsuokai* (Sashida), *Hemicryptocapsa marcucciae* (Cortese), *Hiscocapsa kodrai* (Chiari, Marcucci and Prela), *Praewilliriedellum convexum* (Yao), *Protunuma turbo* Matsuoka, *Semihsuum amabile* (Aita), *Unuma gordus* Hull, *Williriedellum formosum* (Chiari, Marcucci and Prela), *Zhamoidellum* sp. aff. *Z. ventricosum* Dumitrica.

Age: latest Bajocian-early Bathonian to late Bathonian-early Callovian (UAZ 5-7) for the occurrence of *Eucyrtidiellum semifactum* Nagai and Mizutani with *Semihsuum amabile* (Aita) and *Protunuma turbo* Matsuoka.

f) Gurth 2

G2-1: *Eucyrtidiellum dentatum* Baumgartner, *Protunum*a sp. cf. *P. lanosus* Ozvoldova, *Quarkus* sp. cf. *Q. madstonense* (Pessagno, Blome and Hull), *Theocapsommella cucurbiformis* (Baumgartner), *Theocapsommella medvednicensis* (Goričan).

Age: latest Bajocian-early Bathonian to late Bathonian-early Callovian (UAZ 5-7) for the co-occurrence of *Eucyrtidiellum dentatum* Baumgartner with *Theocapsomella cucurbiformis* (Baumgartner).

G2-2: *Hemicryptocapsa marcucciae* (Cortese), *Hemicryptocapsa yaoi* (Kozur), *Praewilliriedellum convexum* (Yao), *Striatojaponocapsa synconexa* O'Dogherty, Goričan and Dumitrica, *Striatojaponocapsa* sp. cf. *S. synconexa* O'Dogherty, Goričan and Dumitrica, *Transhsuum* sp., *Unuma gordus* Hull, *Zhamoidellum* sp. 2 sensu O'Dogherty et al. (2006).

Age: late Bajocian to late Bathonian-early Callovian **(UAZ 4-7)** for the co-occurrence of *Hemicryptocapsa marcucciae* (Cortese), *Unuma gordus* Hull with *Striatojaponocapsa synconexa* O'Dogherty, Goričan and Dumitrica.

G2-3: *Hemicryptocapsa yaoi* (Kozur), *Striatojaponocapsa conexa* (Matsuoka), *Striatojaponocapsa synconexa* O'Dogherty, Goričan and Dumitrica, *Zhamoidellum* sp.

Age: late Bajocian to late Bathonian-early Callovian **(UAZ 4-7)** for the presence of *Striatojaponocapsa conexa* (Matsuoka) with *Striatojaponocapsa synconexa* O'Dogherty, Goričan and Dumitrica.

Considering the stratigraphic position of the samples we could assign an UAZ 5-7 age to the samples G2-1, G2-2 and G2-3 (latest Bajocian-early Bathonian to late Bathonian-early Callovian).

g) Gurth 4

G4-1: *Archaeodictyomitra* sp. cf. *A. rigida* Pessagno, *Eucyrtidiellum pustulatum* Baumgartner, *Helvetocapsa matsuokai* (Sashida), *Hiscocapsa kodrai* (Chiari, Marcucci and Prela), *Striatojaponocapsa synconexa* O'Dogherty, Goričan and Dumitrica, *Unuma gordus* Hull.

Age: latest Bajocian-early Bathonian to late Bathonian-early Callovian **(UAZ 5-7)** for the presence of *Eucyrtidiellum pustulatum* Baumgartner with *Striatojaponocapsa synconexa* O'Dogherty, Goričan and Dumitrica.

G4-3 *Eucyrtidiellum semifactum* Nagai and Mizutani, *Helvetocapsa matsuokai* (Sashida), *Hemicryptocapsa* sp. cf. *H. buekkense* (Kozur), *Protunuma lanosus* Ozvoldova, "*Tricolocapsa*" *tetragona* Matsuoka, *Unuma gordus* Hull, *Unuma latusicostatus* (Aita), *Zhamoidellum* sp. aff. *Z. ventricosum* Dumitrica.

Age: latest Bajocian-early Bathonian (UAZ 5) for the occurrence of *Eucyrtidiellum semifactum* Nagai and Mizutani, "*Tricolocapsa*" *tetragona* Matsuoka and *Unuma latusicostatus* (Aita).

Considering the stratigraphic position of the samples the age of the sample G4-1 could be referable to the UAZ 5 (latest Bajocian-early Bathonian)

DISCUSSION AND CONCLUSIONS

The examined radiolarian cherts yielded radiolarians with moderate to good preservation and the determined age spanning from UAZ 4-5 to UAZ 5-7. In the sub-ophiolitic mélange (Rubik Complex) the oldest ages of radiolarian associated with the basalts (Fig. 9) are referable to the UAZ 4-5 (late Bajocian to latest Bajocian-early Bathonian; sample AL371, Karma 1 section) and UAZ 5 (latest Bajocian-early Bathonian; sample AL372**,** Karma 2 section). Similar ages were found in the radiolarian cherts belonging to the Eastern Mirdita ophiolites (Fig. 9), the samples collected in the Gurth 4 section (G4-1 and G4-3 samples) were assigned to UAZ 5 (latest Bajocian-early Bathonian) and the samples collected in the Gurth 2 section (G2-1 G2-2 and G2-3 samples) indicated an UAZ 5-7 age (latest Bajocian-early Bathonian to late Bathonian-early Callovian). Finally, the ages of the samples, GU7 and GU8 collected in the Gurth section are respectively UAZ 5-6 (latest Bajocian-early Bathonian to middle Bathonian) and UAZ 5-7 ages (latest Bajocian-early Bathonian to late Bathonian-early Callovian).

It is worth of note that the oldest published age of the sub-ophiolitic mélange is refereable to Late Anisian-Early Ladinian as indicated in Chiari et al. (1996), anyway in the present work we obtained more precise Jurassic ages for the radiolarian cherts belonging to this mélange. In fact, Kellici et al. (1994) indicated late Bajocian to late Bathonian-early Callovian and middle Bathonian to late Bathonian-early Callovian ages (UAZ 4-7 and UAZ 6-7 in Bortolotti et al., 2013). Considering the new data of the Eastern Mirdita ophiolites (UAZ 5, UAZ 5-6) these ages are comparable with the published ages reported in Chiari et al. (1994; 2002), Bortolotti et al. (2013) for Fushe Arrez (UAZ 4-5, late Bajocian to latest Bajocian-early Bathonian) and Shebaj (UAZ 5, latest Bajocian-early Bathonian).

Unfortunately, due to the intense alteration of the volcanic rocks associated with the studied radiolarian cherts it was not possible to assess the geochemical nature of the volcanic events occurring in these times. For the EMO, regional comparison and previous works show that the age ranges found in this study (namely, latest Bajocian-early Bathonian to late Bathonian-early Callovian) can be referred to an IAT magmatic activity (Chiari et al., 1994; 2002; Bortolotti et al., 2013). In contrast, for what concerns the sub-ophiolitic mélange in the WMO, no literature data showing clear relationships between radiolarian biostratigraphy and geochemical affinity of stratigraphically associated volcanic rocks are available in literature. Nonetheless, datings of basaltic rocks using radiolarian biostratigraphy are available for the volcanic series of the WMO sequences (Marcucci et al., 1994; Prela et al., 2000; Chiari et al., 2002). These data show that latest Bajocian to

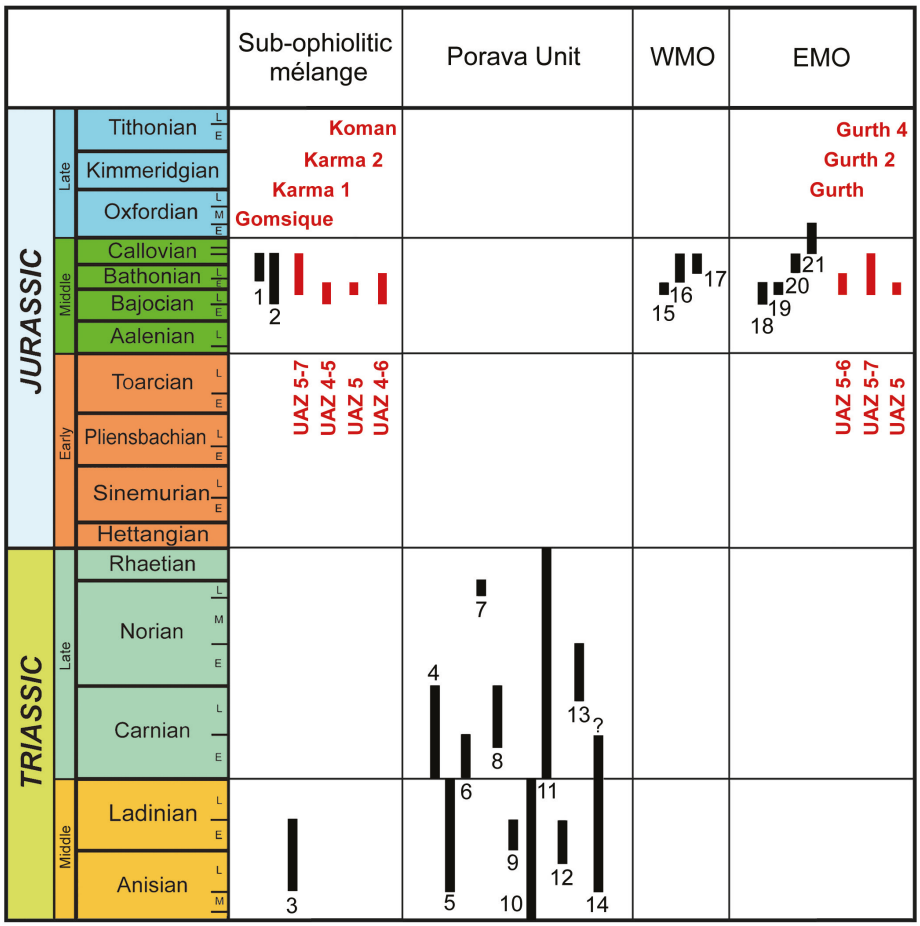

Fig. 9 - Ages of the radiolarian cherts in the Mirdita ophiolites (WMO: Western Mirdita Ophiolites, EMO: Eastern Mirdita ophiolites) and sub-ophiolitic mélange in north Albania. The ages of the Triassic Porava Unit are also shown for comparison (modified from Bortolotti et al., 2013). 1-2) Kellici et al. (1994), Bortolotti et al. (2013); 3) Chiari et al. (1996); 4) Kellici et al. (1994); 5) Marcucci et al. (1994); 6-9) Chiari et al. (1996); 10-11) Bortolotti et al. (2004); 12-13) Bortolotti et al. (2006); 14) Gawlick et al. (2008); 15-17) Prela et al. (2000); 18-19) Chiari et al. (1994); 20-21) Marcucci et al. (1994); Red bars: this study.

early Callovian radiolarian ages in the WMO can always be referred to an N-MORB type magmatic activity. In the absence of any data from both this paper and from literature, we therefore speculate that the late Bajocian to latest Bajocian-early Bathonian and latest Bajocian-early Bathonian to late Bathonian-early Callovian ages found in this paper could also be referred to an N-MORB magmatic activity. Nonetheless, future investigations on volcanic rocks-radiolarian chert pairs within the sub-ophiolitic mélanges of both the WMO and EMO should be carried out to fill this void of data. The commonly accepted geodynamic reconstructions of the Jurassic evolution of the Albanian Neo-Tethys implies that the N-MORB magmatism in the WMO formed, together with the MTB magmatism, during the very early stages of subduction initiation (nascent arc). Subduction then shortly evolved to a relatively mature stage with the formation of a mature intra-oceanic arc where IAT and boninitic sequences of the EMO formed (Saccani et al., 2004; 2011; 2017; Dylek et al., 2005; 2007; 2008; Bortolotti et al., 2013; van Hinsbergen et al., 2020). The new age data obtained in this work are well consistent with this geodynamic reconstruction; in fact, we suggest that radiolarian cherts in the sub-ophiolitic mélange of the WMO date the nascent arc stage of the subduction, whereas the slightly younger ages found in the EMO date the subsequent mature stage of the subduction. Hower the literature biostratigraphic data show that no significant age differences in age exist between the nascent arc stage and mature subduction.

ACKNOWLEDGEMENTS

We would thanks Michele Marroni and Špela Goričan for their useful suggestions and remarks. The radiolarian micrographs were taken by Maurizio Ulivi and Laura Chiarantini with a ZEISS EVO MA15 of the M.E.M.A (University of Florence). This research has been funded by FAR-2022 project of the Ferrara University (head E.S.).

References

Auer M., Gawlick H.J., Suzuki H. and Schlagintweit F., 2009. Spatial and temporal development of siliceous basin and shallow-water carbonate sedimentation in Oxfordian Northern Calcareous Alps. Facies, 55: 63-87.

Baumgartner P.O., Bartolini A., Carter E.S., Conti M, Cortese G., Danelian T., De Wever P., Dumitrica P., Dumitrica-Jud R., Goričan Š., Guex J., Hull D.M., Kito N., Marcucci M., Matsuoka A., Murchey B., O'Dogherty L., Savary J., Vishnevskaya V., Widz D. and Yao A., 1995. Middle Jurassic to Early Cretaceous Radiolarian biochronology of Tethys based on Unitary Associations. In: Baumgartner P.O, O'Dogherty L., Goričan Š., Urquhart E., Pillevuit A. and De Wever P. (Eds.), Middle Jurassic to Lower Cretaceous Radiolaria of Tethys: occurrences, systematics, biochronology. Mém. Géol. Lausanne, 23: 1013-1048.

Bébien J., Dimo-Lahitte A., Vergély P., Insergueix-Filippi D. and Dupeyrat L., 2000. Albanian ophiolites. I - Magmatic and metamorphic processes associated with the initiation of a subduction. Ofioliti, 25: 39-45.

Bébien J., Shallo M., Manika K. and Gega D., 1998. The Shebenik Massif (Albania): A link between MOR- and SSZ-type ophiolites. Ofioliti, 23: 7-15.

Beccaluva L., Coltorti M., Premti I., Saccani E., Siena F. and Zeda O., 1994, Mid-Ocean ridge and suprasubduction affinities in the ophiolitic belts from Albania. Ofioliti, 19: 77-96.

Beccaluva L., Coltorti, M., Saccani E. and Siena F., 2005. Magma generation and crustal accretion as evidenced by supra-subduction ophiolites of the Albanide-Hellenide Subpelagonian zone. Isl. Arc., 14: 551-563.

Bortolotti V., Carras N., Chiari M., Fazzuoli M., Marcucci M., Photiades A. and Principi G., 2003. The Argolis Peninsula in the palaeogeographic and geodynamic frame of the Hellenides. Ofioliti, 28 (2): 79-94.

Bortolotti V., Chiari M., Gonçuoğlu M.C., Principi G., Saccani E., Tekin U.K. and Tassinari R., 2018. The Jurassic-Early Cretaceous basalt-chert association in the ophiolites of the Ankara Mélange, east of Ankara, Turkey: age and geochemistry. Geol. Mag., 155: 451-478.

Bortolotti V., Chiari M., Kodra A., Marcucci M., Marroni M., Mustafa F., Prela M., Pandolfi L., Principi G. and Saccani E., 2006. Triassic MORB magmatism in the southern Mirdita zone (Albania). Ofioliti, 31: 1-9.

Bortolotti V., Chiari M., Kodra A., Marcucci M., Mustafa F., Principi G. and Saccani E., 2004. New evidence for Triassic MORB magmatism in the northern Mirdita Zone ophiolites (Albania). Ofioliti, 29: 243-246.

Bortolotti V., Chiari M., Marroni M., Pandolfi L., Principi G. and Saccani E., 2013. The geodynamic evolution of the ophiolites from Albania and Greece, Dinaric-Hellenic belt: One, two or more oceanic basins?. Intern. J. Earth Sci., 102: 783-811.

Bortolotti V., Chiari M., Marcucci M., Photiades A., Principi G. and Saccani E., 2008. New geochemical and age data on the ophiolites from the Othrys area (Greece): Implication for the Triassic evolution of the Vardar Ocean. Ofioliti, 33: 135-151.

Bortolotti V., Kodra A., Marroni M., Mustafa F., Pandolfi L., Principi G. and Saccani E., 1996. Geology and petrology of ophiolitic sequences in the Mirdita region (Northern Albania). Ofioliti, 21: 3-20.

Bortolotti V., Marroni M., Pandolfi L., Principi G. and Saccani E., 2002. Interaction between mid-ocean ridge and subduction magmatism in Albanian ophiolites. J. Geol., 110: 561-576.

Carosi R., Cortesogno L., Gaggero L. and Marroni M., 1996. Geological and petrological features of the metamorphic sole from the Mirdita ophiolites, northern Albania. Ofioliti, 21: 21-40.

Carter E.S., Goričan Š., Guex J., O'Dogherty L., De Wever P., Dumitrica P., Hori R.S., Matsuoka A. and Whalen P.A., 2010. Global radiolarian zonation for the Pliensbachian, Toarcian and Aalenian: the link between zonations for the Lower Jurassic (Hettangian-Sinemurian) and the Middle and Upper Jurassic. Palaeo. Palaeo. Palaeo., 297: 401-419.

Chiari M., Bortolotti V., Marcucci M., Photiades A., Principi G. and Saccani E., 2012. Radiolarian biostratigraphy and geochemistry of the Koziakas Massif ophiolites (Greece). Bull. Soc. Géol. Fr., 183 (4): 287-306.

Chiari M., Cobianchi M. and Picotti V., 2007. Integrated stratigraphy (radiolarians and calcareous nannofossils) of the Middle to Upper Jurassic Alpine radiolarites (Lombardian Basin, Italy): constraints to their genetic interpretation. Palaeo. Palaeo. Palaeo., 249: 233-270.

Chiari M., Di Stefano P. and Parisi G., 2008. New stratigraphic data on the Middle-Late Jurassic biosiliceous sediments from the Sicanian basin, Western Sicily (Italy). Swiss J. Geosci., 101: 415-429.

Chiari M., Marcucci M., Cortese G., Ondrejickova A. and Kodra A., 1996. Triassic radiolarian assemblages in the Rubik area and Cukali zone, Albania. Ofioliti, 21: 77-84

Chiari M., Marcucci M. and Prela M., 1994. Mirdita ophiolites Project: 2- Radiolarian assemblages in the cherts at Fushe Arrez and Shebaj (Mirdita area, Albania). Ofioliti, 19 (2a): 313-318.

Chiari M., Marcucci M. and Prela M., 2002. New species of Jurassic radiolarian in the sedimentary cover of ophiolites in the Mirdita area, Albania. Micropaleontology, 48: 61-87.

Chiari M., Marcucci M. and Prela M., 2004. Radiolarian assemblages from the Jurassic cherts of Albania: new data. Ofioliti, 29: 95-105.

Crawford A.J., Falloon A. and Green D.H., 1989. Classification, petrogenesis and tectonic setting of boninites, In: A.J. Crawford (Ed.), Boninites and related rocks. London, Unwin Hyman, p. 1-49.

Danelian T., De Wever P. and Durand-Delga M., 2008. Revised radiolarian ages for the sedimentary cover of the Balagne ophiolite (Corsica, France). Implications for the palaeoenvironmental evolution of the Balano-Ligurian margin. Bull. Soc. Géol. Fr., 179 (3): 289-296

Dilek Y. and Furnes H., 2009, Structure and geochemistry of Tethyan ophiolites and their petrogenesis in subduction rollback systems. Lithos, 113: 1-20.

Dilek Y., Furnes H. and Shallo M., 2007. Suprasubduction zone ophiolite formation along the periphery of Mesozoic Gondwana. Gondw. Res., 11: 453-475.

Dilek Y., Furnes H. and Shallo M., 2008. Geochemistry of the Jurassic Mirdita Ophiolite (Albania) and the MORB to SSZ evolution of a marginal basin oceanic crust. Lithos, 100: 174-209.

Dilek Y., Shallo M. and Furnes H., 2005. Rift-drift, seafloor spreading, and subduction tectonics of Albanian ophiolites. Intern. Geol. Rev., 47: 147-176.

Dumitrica, P. and Dumitrica-Jud, R., 2005. *Hexasaturnalis nakasekoi* nov. sp., a Jurassic saturnalid radiolarian species frequently confounded with *Hexasaturnalis suboblongus* (Yao). Rev. Micropal.. 48: 159-168.

Ferrière J., Chanier F. and Ditbanjong P., 2012, The Hellenic ophiolites: eastward or westward obduction of the Maliac Ocean, a discussion. Intern. J. Earth Sci., 101: 1559-1580.

Gaggero L., Marroni M., Pandolfi L. and Buzzi L., 2009. Modelling of oceanic lithosphere obduction: constraints from the metamorphic sole of Mirdita ophiolites (Northern Albania). Ofioliti, 34: 17-43.

Gawlick H.J., Frisch W., Hoxha L., Dumitrica P., Krystyn L., Lein R., Missoni S. and Schlagintweit F., 2008. Mirdita Zone ophiolites and associated sediments in Albania reveal Neotethys Ocean origin. Intern. J. Earth Sci., 97: 865-881

Gawlick H.J., Goričan Š., Missoni S., Dumitrica P., Lein R. Frisch W. and Hoxha L., 2016. Middle and Upper Triassic radiolarite components from the Kcira-Dushi-Komani ophiolitic mélange and their provenance (Mirdita Zone, Albania). Rev. Micropal., 59 (4): 359-380.

Gawlick H.J., Missoni S., Sudar M.N., Suzuki H., Méres Š., Lein R. and Jovanovic D., 2018. The Jurassic Hallstatt Mélange of the Inner Dinarides (SW Serbia): implications for Triassic-Jurassic geodynamic and palaeogeographic reconstructions of the Western Tethyan realm. N. Jahr. Geol. Palaont. Abhandl., 288 (1): 1-47.

Goričan Š., Pavšič J. and Rožič B., 2012. Bajocian to Tithonian age of radiolarian cherts in the Tolmin Basin (NW Slovenia). Bull. Soc. Géol. Fr., 183 (4): 369-382.

Halamić J., Goričan Š., Slovenec D. and Kolar-Jurkovšek T., 1999. Middle Jurassic radiolarite-clastic succession from the Medvednica Mt. (NW Croatia). Geol. Croatica, 52: 29-57.

Hoeck V., Koller F., Meisel T., Onuzi K. and Kneringer E., 2002. The Jurassic South Albanian ophiolites: MOR- vs. SSZ-type ophiolites. Lithos, 65: 143-164.

Hoeck V., Ionescu C. and Onuzi K., 2014. The Southern Albanian ophiolites. CBGA 2014 Field Trip FT5. Bul. Shkenc. Gjeol., 7/2014, Spec. Iss., 48 pp.

Insergueix-Filippi D., Dupeyrat L., Dimo-Lahitte A., Vergely P. and Bébien J. 2000. Albanian ophiolites. II - Model of subduction zone infancy at a mid-ocean ridge. Ofioliti, 25: 47-53.

Jones G., De Wever P. and Robertson A.H.F., 1992. Significance of radiolarian age data to the Mesozoic tectonic and sedimentary evolution of the northern Pindos Mountains, Greece. Geol. Mag., 129: 385-400.

Kellici I., De Wever P. and Kodra A., 1994. Radiolaires mésozoïques du massif ophiolitique de Mirdita nappe, Albanie. Paléontologie et stratigraphie. Rev. Micropal., 37: 209-222.

Koller F., Hoeck V., Meisel T., Ionescu C., Onuzi K. and Ghega D., 2006. Cumulates and gabbros in southern Albanian ophiolites: their bearing on regional tectonic setting. In: A.H.F. Robertson and D. Mountrakis (Eds.), Tectonic development of the Eastern Mediterranean Region. Geol. Soc. London Spec. Publ., 260: 267-299.

Manika K., Shallo M., Bébien J. and Gega D., 1997. The plutonic sequence of Shebenik ophiolite complex, Albania: evidence for dual magmatism. Ofioliti, 22: 93-99.

Marcucci M. and Prela M., 1996. The Lumi i zi, (Puke) section of the Kalur Cherts: Radiolarian assemblages and comparison with other sections in Northern Albania: Ofioliti, 21: 71-76.

Marcucci M., Kodra A., Pirdeni A. and Gjata Th., 1992. Radiolarian assemblages in the Triassic and Jurassic cherts of Albania. Working Group Meeting, IGCP 256, Tirana, October 1992, Abstr., p. 33-34.

Marcucci M., Kodra A., Pirdeni A. and Gjata T., 1994. Radiolarian assemblages in the Triassic and Jurassic cherts of Albania. Ofioliti, 19: 105-114.

Matsuoka A., 1983. Middle and Late Jurassic radiolarian biostratigraphy in the Sakawa and adjacent areas, Shikoku, southwest Japan. J. Geosci. Osaka City Univ., 26: 1-48.

Matsuoka A. and Ito T., 2019. Updated radiolarian zonation for the Jurassic in Japan and the western Pacific. Sci. Rep., Niigata Univ. (Geology), 34: 49-57.

Monjoie P., Lapierre H., Tashko A., Mascle G.H., Dechamp A., Muceku B. and Brunet P., 2008. Nature and origin of the Triassic volcanism in Albania and Othrys: a key to understanding the Neotethys opening? Bull. Soc. Géol. Fr., 179: 411-425.

Myhill R., 2011. Constraints on the evolution of the Mesohellenic Ophiolite from subophiolitic metamorphic rocks. In: J. Wakabayashi and Y. Dilek (Eds.), Mélanges processes of formation and societal significance. Geol. Soc. Am. Spec. Pap., 480: 75-94.

O'Dogherty L., Bill M., Goričan Š., Dumitrica P. and Masson H., 2006. Bathonian radiolarians from an ophiolitic melange of the Alpine Tethys (Gets Nappe, Swiss-French Alps). Micropaleontology, 51: 425-485.

O'Dogherty L., Carter E.S., Dumitrica P., Goričan Š., De Wever P., Bandini A.N., Baumgartner P.O. and Matsuoka A., 2009. Catalogue of Mesozoic radiolarian genera. Part 2: Jurassic-Cretaceous. Geodiversitas, 31: 271-356.

O'Dogherty L., Goričan Š. and Gawlick H.J., 2017. Middle and Late Jurassic radiolarians from the Neotethys suture in the Eastern Alps. J. Paleont., 91: 25-72.

Pearce J.A., van der Laan S.R., Arculus R.J., Murton B.J., Ishii T., Peate D.W. and Parkinson I.J., 1992. Boninite and harzburgite from Leg 125 (Bonin-Mariana forearc): a case study of magina genesis during the initial stage of subduction. In: P. Fryer, J.A. Pearce., L.B. Stokking et al. (Eds.), Proceed O.D.P. Sci. Res., 125: 623-659.

Photiades A., Saccani E. and Tassinari R., 2003. Petrogenesis and tectonic setting of volcanic rocks from the Subpelagonian ophiolitic mélange in the Agoriani area (Othrys, Greece). Ofioliti, 28: 121-135.

Prela M., 1994. Mirdita Ophiolites Project: 1: Radiolarian biostratigraphy of the sedimentary cover of the ophiolites in the Mirdita area (Albania): initial data. Ofioliti, 19 (2): 279-286.

Prela M., Chiari M. and Marcucci M., 2000. Jurassic radiolarian biostratigraphy of the sedimentary cover of ophiolites in the Mirdita Area, Albania: new data. Ofioliti, 25: 55-62.

Robertson A.H.F., 1994. Role of the tectonic facies concept in orogenic analysis and its application to Tethys in the Eastern Mediterranean region. Earth Sci. Rev., 37: 139-213.

Robertson A.H.F. and Shallo M., 2000. Mesozoic-Tertiary tectonic evolution of Albania in its regional Eastern Mediterranean context. Tectonophysics, 316: 197-214.

Saccani E., 2015. A new method of discriminating different types of post-Archean ophiolitic basalts and their tectonic significance using Th-Nb and Ce-Dy-Yb systematics. Geosci. Front., 6: 481-501.

Saccani E. and Photiades A., 2005. Petrogenesis and tectono-magmatic significance of volcanic and subvolcanic rocks in the Albanide-Hellenide ophiolitic mélanges. Isl. Arc, 14: 494-516.

Saccani E. and Tassinari R., 2015. The role of MORB and SSZ magma-types in the formation of jurassic ultramafic cumulates in the Mirdita ophiolites (Albania) as deduced from chromian spinel and olivine chemistry. Ofioliti, 40: 37-56.

Saccani E., Beccaluva L., Coltorti M. and Siena F., 2004, Petrogenesis and tectono-magmatic significance of the Albanide-Hellenide ophiolites. Ofioliti, 29: 77-95.

Saccani E., Beccaluva L., Photiades A. and Zeda O., 2011. Petrogenesis and tectono-magmatic significance of basalts and mantle peridotites from the Albanian–Greek ophiolites and subophiolitic mélanges. New constraints for the Triassic-Jurassic evolution of the Neo-Tethys in the Dinaride sector. Lithos, 124: 227-242 .

Saccani E., Dilek Y. and Photiades A., 2017 Time-progressive mantle-melt evolution and magma production in a Tethyan marginal sea: A case study of the Albanide-Hellenide ophiolites. Lithosphere, 10: 35-53.

Šegvić B., Kukoč D., Dragičević I., Vranjković A., Brčić V., Goričan Š., Babajić E. and Hrvatović H., 2014. New record of Middle Jurasisic radiolarians and evidence of Neotethyan dynamics documented in a mélange from the central Dinaric ophiolite belt (CDOB, NE Bosnia and Herzegovina). Ofioliti, 39 (1): 31-41

Shallo, M. 1994. Outline of the Albanian ophiolites. Ofioliti, 19: 57-75.

Shallo M. and Dilek Y., 2003, Development of the ideas on the origin of Albanian ophiolites. In: Y. Dilek and S. Newcomb (Eds.), ophiolite concept and the evolution of geological thought. Geol. Soc. Am. Spec. Pap., 373: 351-364.

Shallo M., Kote D. and Vranaj A., 1987. Geochemistry of the volcanics from ophiolitic belts of Albanides. Ofioliti, 12: 125-136.

Shervais J.W., 1982. Ti-V plots and the petrogenesis of modern ophiolitic lavas: Earth Planet. Sci. Lett., 59: 101-118.

Šmuc A. and Goričan Š., 2005. Jurassic sedimentary evolution of a carbonate platform into a deep-water basin, Mt. Mangart (Slovenian-Italian border). Riv. It. Pal. Strat. 111:45-70.

Sun S.S. and McDonough W.F., 1989. Chemical and isotopic systematics of ocean basalts: Implications for mantle composition and processes. In: A.D. Saunders and M.J. Norry (Eds.), Magmatism in the ocean basins: Geol. Soc. London Spec. Publ., 42: 313-346.

van Hinsbergen D.J.J., Torsvik T.H. Schmid S.M. Matenco L.C., Maffione M., Gürer D. and Vissers R.L.M., Gürer D. and Spakman W., 2020. Companion paper. Orogenic architecture of the Mediterranean region and kinematic reconstruction of its tectonic evolution since the Triassic. Gondw. Res., 81: 79-229.

Workman R.K. and Hart S.R., 2005, Major and trace element composition of the depleted MORB mantle (DMM): Earth Planet. Sci. Lett., 231: 53-72.

Xhomo A, Kodra A, Dimo, L. et al., 2002. Geological Map of Albania 1: 200.000 scale. Geol. Surv. of Albania, Republika e Shqiperise.

Received, June, 2, 2023
Accepted, July 10, 2023